

**Physiological significance of ATP and
glutamate release from astrocytes**

Hae Ung Lee

**DOCTOR OF
PHILOSOPHY**

Department of Physiological Sciences
School of Life Science
The Graduate University for Advanced Studies

2008

**Physiological significance of ATP and
glutamate release from astrocytes**

Hae Ung Lee

Submitted in partial fulfillment of the
Requirements for the degree
of Doctor in Philosophy
Department of Physiological Sciences
School of Life Science
The Graduate University for Advanced Studies

Abstract

Astrocytes, the major glial cell type in the CNS, have been considered to be passive bystanders that merely provide support to neuronal networks. However astrocyte is now recognized as one of the active elements that directly modulate brain functions. Astrocytes sense and integrate synaptic activity and, depending on intracellular Ca^{2+} levels, release gliotransmitters (e.g. glutamate, ATP and D-serine) that have feedback actions on neurons. Although these reports provided clues that astrocytes are the active components in the brain, they did not analyze the temporal and spatial pattern of gliotransmitters release from astrocytes. To examine the release of gliotransmitters, such as ATP and glutamate, I applied imaging techniques visualizing ATP and glutamate released from astrocytes.

Luciferin-luciferase solution was applied to the extracellular fluid of astrocytes to visualize ATP release. To visualize glutamate release, glutamate optic sensor (EOS) was applied. This specific probe for detecting glutamate is a hybrid molecule consisting of glutamate-binding protein (AMPA receptor GluR2 subunit extracellular domain as a glutamate-binding protein) and a small-molecule fluorescent dye. I successfully observed ATP or glutamate release from astrocytes and applied these technologies to observe spatial and temporal pattern of gliotransmitters release.

Many researchers found that the astrocytic intracellular calcium responses are co-related with the functions of astrocytes. To reveal the significance of intracellular calcium elevation of astrocytes on the gliotransmitter release, I tried to obtain the spatio-temporal information using these technologies combined with

the calcium imaging technology. By ATP (1 μ M or higher) stimulation, intracellular calcium elevation was observed in all astrocytes. However, under the same condition, only few astrocytes (ca. 3~7%) released glutamate. A similar phenomenon was observed in glutamate-evoked ATP release from astrocytes; even though all astrocytes showed increased intracellular calcium levels, small proportion of astrocytes released ATP by glutamate stimulation (ca. 1%). It was expected that astrocytes which showed intracellular calcium elevation release gliotransmitters, however, my results were totally different.

Pharmacological approaches revealed that P2X and P2Y receptors showed different patterns of intracellular calcium elevation, however, a similar pattern of glutamate release was evoked by P2X and P2Y stimulations. For the glutamate stimulation, it was suggested that the subtype 5 of metabotropic glutamate receptor was responsible to increase intracellular calcium in astrocytes and to release ATP from astrocytes. The glutamate stimulation evoked calcium waves among astrocytes, and then astrocytes released ATP around 200 seconds after glutamate application.

My experiments using cultured astrocytes revealed following things: 1) intracellular calcium elevation was not enough to evoke gliotransmitter release, 2) direct relationship between glutamate release and intracellular calcium elevation evoked by ATP stimulation is low, 3) ATP release evoked by glutamate stimulation had relevance to the intracellular calcium elevation which represent the activation of astrocytes. For the first time, gliotransmitter release was successfully visualized and the mechanisms of gliotransmitter release were revealed through these imaging technologies.

Table of Contents

Table of Contents	4
List of Figures	6
List of Tables	6
List of Abbreviations	7
Acknowledgements	8
I. Introduction.....	10
A. Structural and Physiologic properties of astrocytes	10
B. Classification of astrocytes	12
C. Function of astrocytes.....	13
1. Ion Homeostasis	13
2. Transmitter Removal.....	15
3. Metabolic Coupling with Neurons.....	16
D. Purinergic receptors expressed in astrocytes	18
E. Glutamate receptors expressed in astrocytes	19
F. Calcium Waves of astrocytes	20
G. Gliotransmitters	21
1. The Concept of Gliotransmission.....	21
2. Regulation of synaptic activity by astrocytic glutamate release.....	22
3. Regulation of synaptic activity by astrocytic ATP release	23
4. Mechanisms of gliotransmitters release.....	24
5. Spatial-temporal characteristics of ATP and glutamate release in astrocytes	25
Thesis Aims	27
II. Materials and Methods	29
A. Solutions and chemicals.....	29
B. Cell preparation	30
C. Perfusing chamber for measuring extracellular ATP and glutamate concentration released from astrocytes	31
D. Luciferin-luciferase ATP assay.....	32
E. Assay of glutamate release.	32
F. Visualization of intracellular calcium dynamics in cultured astrocytes..	33
G. Visualization of ATP dynamics in cultured astrocytes.....	34
H. Visualization of glutamate dynamics in cultured astrocytes.....	34
III. Results.....	36
A. Extracellular concentration of ATP and glutamate released from astrocytes	36
B. New technologies to visualize ATP and glutamate release from astrocytes	37
C. Evaluation of ATP imaging system	38
D. Evaluation of glutamate imaging system	39
E. The cell culture condition to observe ATP and glutamate release evoked by physiological stimulation.....	40
F. ATP and glutamate release evoked by physiological stimulation	41
G. Intracellular calcium elevation of astrocytes by ATP stimulation	42

H. Effect of purinergic receptor antagonist on the intracellular calcium levels in astrocytes.....	43
I. Analysis of spatial and temporal information of ATP-evoked glutamate release in astrocytes	44
J. Effect of purinergic receptors antagonists on glutamate release evoked by ATP	45
K. Glutamate increased astrocytic intracellular calcium levels only at a high concentration	46
L. Effect of glutamate receptors antagonists to intracellular calcium elevation	47
M. Analysis of spatial and temporal information of glutamate-evoked ATP release in astrocytes	48
N. Effect of glutamate receptors antagonists on ATP release evoked by glutamate	49
IV. Discussion	51
A. The responses of the intracellular calcium elevation in astrocytes which I prepared in my serial experiments	51
B. Pharmacological properties of ATP-evoked astrocytic intracellular calcium elevation.....	53
C. Property of ATP-evoked glutamate release from astrocytes	54
D. Differences in the dynamics between hypotonic stress-evoked and ATP-evoked glutamate release	56
E. Pharmacological properties of glutamate-evoked astrocytic intracellular calcium elevation.....	58
F. Property of glutamate-evoked ATP release from astrocytes	60
G. Heterogeneity of ATP and glutamate release in astrocytes	61
H. Release machineries of gliotransmitters	62
I. Further studies on ATP and glutamate imaging.....	63
V. References.....	65
Figure Legends.....	85

List of Tables:

Table 1: Number of cells that showed increased level of intracellular calcium by purinergic and glutamate receptors agonists stimulation.....	81
Table 2: Effect of purinergic and glutamate receptor antagonists to intracellular calcium elevation.....	82
Table 3: Glutamate release from astrocytes.....	83
Table 4: Effect of purinergic receptor antagonists on glutamate release evoked by ATP	84

List of Figures

Figure 1 Concentrations of extracellular ATP or glutamate released from astrocytes	96
Figure 2 New technologies to visualize ATP and glutamate release	97
Figure 3 Evaluation of ATP imaging.	98
Figure 4 Evaluation of Glutamate imaging	99
Figure 5 Intracellular calcium elevation of astrocytes by ATP or glutamate stimulation.	100
Figure 6 Effect of purinergic receptor antagonists on the intracellular calcium levels in astrocytes evoked 1 μM ATP stimulation	101
Figure 7 Effect of purinergic receptor antagonists on the intracellular calcium levels in astrocytes evoked by 10 μM ATP stimulation.....	102
Figure 8 Imaging analysis of glutamate release from astrocyte evoked by 1 μM ATP.....	103
Figure 9 Imaging analysis of glutamate release from astrocytes evoked by 10 μM ATP.....	104
Figure 10 Intracellular calcium elevation of astrocytes by ATP or glutamate stimulation.	105
Figure 11 Effect of glutamate receptor antagonist (MPEP) to intracellular calcium elevation.....	106
Figure 12 Effect of glutamate receptor antagonists (CNQX and AP5) to intracellular calcium elevation.....	107
Figure 13 Analysis of ATP imaging.....	108
Figure 14 Effect of metabotropic glutamate receptor antagonist, MPEP on ATP release evoked by glutamate	109
Figure 15 Effect of AMPA receptor antagonist, CNQX on ATP release evoked by glutamate	110
Figure 16 Effect of NMDA receptor antagonist, AP5 on ATP release evoked by glutamate	111
Figure 17 Combination analysis of calcium imaging and glutamate imaging evoked by ATP stimulation	112
Figure 18 Scheme of glutamate release from astrocytes	113
Figure 19 Combination analysis of calcium imaging and ATP imaging evoked by glutamate stimulation	114

Abbreviations used:

ADP: Adenosine diphosphate

AMPA: α -amino-3-hydroxy-5-methyl-4-isoxazolepropionic acid

AP5 (or APV): (2R)-amino-5-phosphonovaleric acid

ATP: Adenosine 5'-triphosphate

ATP γ S: adenosine 5'-(gamma-thio) triphosphate

CHPG: (R,S)-2-chloro-5-hydroxyphenylglycine 2-amino-2-(2-chloro-5-hydroxy-phenyl) acetic acid

CNQX: 6-cyano-7-nitroquinoxaline-2, 3-dione

EAAT: excitatory amino acid transporters

ECS: extracellular space

EOS: glutamate optic sensor

GFAP: Glial fibrillary acidic protein

mGluR: metabotropic glutamate receptor

MPEP: 6-methyl-2-(phenylethynyl) pyridine

NAD: nicotinamide adenine dinucleotide

NMDA: N-methyl-D-aspartic acid

PPADS: Pyridoxal-phosphate-6-azophenyl-2',4'-disulfonic acid

UTP: Uridine triphosphate

Acknowledgements

To Professor Kazuhiro Ikenaka, for his support and help all these years. For his generosity in letting me study in NIPS which is one of the brilliant institutes in the world. For three years, he has taught many things from basis of researches. He's always surprised me with his knowledge, wit and enthusiasm for knowing something. I'm sure he can make himself understood what I write in next sentence in Korean. “선생님을 만난 것은 제 인생의 가장 큰 행운이었습니다. 감사합니다.”

To Dr. Kenji Tanaka. For only one month, he had left many things inside me before he studied in N.Y. After his coming back here last year, I discussed many things with him thoroughly as if I had wanted to compensate two years. It was my pleasure to discuss with him. He was my teacher and friend to share everything include problems. I feel very fortunate for having been able to work with him. I always appreciate his kindness.

To Dr. Koji Shibasaki. He was one of the members of Ikenaka lab. It always makes me easy to ask anything to him. He is one of my mentors who always have inspired me. Thank you for your kindness. To Dr. Masae Naruse, she took care of me when I first came here. I really appreciated her help.

To Professor Yasunobu Okada, I learned many things from his lab. I thank for his support. In his lab, I met Dr. Hongtao Liu who taught me cell culture and electrophysiology. It was the start of my research life in new field. It was great

challenge for me to do electrophysiology. He was a talented person. Without his help, I could not do anything. Thank you for your kindness.

In Nagoya I met an amazing group of people. Professor Kenzo Hirose amazed me with his talent and enthusiasm. I really appreciate his support and it was my fortune to work in his lab. They helped me start imaging technology and it was the new world for me. I could overcome the problems with Dr. Shigeyuki Namiki as if he knew everything. I have never seen a talented person like him. It was my pleasure working with him. Working with him always made me improve myself. I'm looking forward to working our next project with him.

It was great experience for me to work with many brilliant researchers. In Nagoya I met another great researcher, Dr. Kishio Furuya who always amazed me during the experiment. But, not only about science, is he friendly and tender. It was my good memory coming back to Okazaki with him. I appreciate his kindness.

To Professor Masahiro Sokabe, he generously allowed me to work in his lab. That was my start of finishing my PhD thesis. I thank for his support.

To my family, Nam-Kyoung for being with me since the first day I arrived to Okazaki where is totally different from Seoul in Korea. For her love and for sharing her life with me. To my parents and my brother for always being there. To my little baby, Seo Reen, I can't forget the first day we met. I love you.

I. Introduction

A. Structural and Physiologic properties of astrocytes

Astrocytes are a sub-type of the glial cells in the brain and spinal cord. They are also known as astrocytic glial cells. Astrocytes are generally identified histologically as the cells expressing the intermediate filament, glial fibrillary acidic protein (GFAP). Astrocytes have multiple fine processes, which cover the entire surface of intraparenchymal capillaries (Peters et al., 1991) and ensheath virtually every synapse (Rohlmann and Wolff, 1996). Thus, astrocytes are polarized cells with some processes contacting endothelial cells of the capillary or fibroblasts of the pia mater, whereas other processes are intimately intertwined with neuronal processes and synapses.

Astrocytes are strongly coupled to one another by gap junctions (Ransom, 1995), aqueous pores which are permeable to ions and other molecules with a molecular weight less than 1,000. A broad range of biologically important molecules, including nucleotides, sugars, amino acids, small peptides, cAMP, calcium and inositol triphosphate have access to this pathway.

The membrane potential (V_m) of astrocytes is more negative than that of neurons. For example, astrocytes have a V_m of about -85 mV, whereas neuronal membrane potential is about -65 mV. Inwardly rectifying K^+ channels are responsible to set the resting potential of astrocytes (Ransom and Sontheimer,

1992). These channels are voltage sensitive and are open at membrane potentials more negative than about -80 mV, close to the resting potential of astrocytes. One consequence of the high K^+ selectivity of astrocytes, compared to neurons, is that the membrane voltage of astrocytes is more sensitive to changes in extracellular $[K^+]$ ($[K^+]_o$). For example, when $[K^+]_o$ is raised from 4 to 20 mM, astrocytes depolarize by ~25 mV, compared to only ~5 mV for neurons (Kuffler and Nicholls, 1966). This relative insensitivity of neuronal resting potential to changes in $[K^+]_o$ in the “physiologic” range may have emerged as an adaptive feature that stabilizes the resting potential of neurons in the face of the transient increases in $[K^+]_o$ that accompany neuronal activity. In contrast, natural stimulation, such as viewing visual targets of different shapes or orientations, can cause depolarizations of up to 10 mV in astrocytes of the visual cortex (Kelly and Van Essen, 1974). Consequently, it indicates excessive extracellular K^+ was removed by astrocytes.

Neurons and astrocytes do not make functional synaptic or gap junction contacts with one another; therefore, interactions between these cell types must occur via the narrow extracellular space (ECS) between them (Kuffler and Nicholls, 1966). In the mammalian central nervous system, the ECS is a uniform and very small compartment formed by adjacent cell membranes which are, on average, separated approximately by 20 nm. Because of the extreme narrowness of the ECS, molecules released from one cell diffuse almost instantly to adjacent cells. Astrocytes interact with neurons by influencing the contents (e.g., ions, energy metabolites, neurotransmitters, etc.) of the ECS. It has been discovered that astrocytes release and express receptors for a wide range of informational

molecules, including neurotransmitters (Kettenmann and Ransom, 1995). Indeed, astrocytes are in a position to sense and modulate synaptic transmission through the processes that surround synapses.

B. Classification of astrocytes

There are several different ways to classify astrocytes. First, astrocytes can be classified by lineage and antigenic phenotype, even though these classifications are rarely used. These have been established by classic work by Martin and his colleagues in early 1980s on rat optic nerves (Miller et al., 1989). He defined antigenically Ran2⁺, GFAP⁺, FGFR3⁺, A2B5⁻ astrocytes of the postnatal day 7 rat optic nerve as type 1 astrocytes. These can arise from the tripotential glial restricted precursor cells (GRP), but not from the bipotential O2A/OPC (oligodendrocyte - type 2 astrocyte precursor, also called as oligodendrocyte progenitor cell) cells. As mentioned above, antigenically A2B5⁺, GFAP⁺, FGFR3⁻, Ran 2⁻ astrocytes were defined as type 2 astrocytes. These cells can develop *in vitro* from either tripotential GRP (probably via O2A stage) or from bipotential O2A cells or *in vivo* when these progenitor cells are transplanted into lesion sites (but probably not in normal development, at least not in the rat optic nerve). Type-2 astrocytes are the major astrocytic component in postnatal optic nerve cultures that are generated by O2A cells grown in the presence of fetal calf serum but their existence *in vivo* is doubtful (Fulton et al., 1992).

Another classification is the anatomical way. In this way, astrocytes are divided into two groups; protoplasmic and fibrous astrocytes. Astrocytes in the gray matter, called protoplasmic astrocytes, have profuse, short stubby processes that contact blood vessels and the pial surface, and surround neurons. Astrocytic end-feet cover the entire surface of intraparenchymal capillaries (Peters et al., 1991). These end-feet express glucose transporters of the GluT 1 type (Morgello et al., 1995) and are a likely site of glucose uptake. In the gray matter, astrocytic processes ensheath virtually every synapse; the ensheathing membranes constitute about 80% of total membrane surface and are devoid of organelles (Rohlmann and Wolff, 1996). Astrocytes in the white matter are complex cells with 50 to 60 long branching processes that radiate from the cell body and terminate in end-feet at the pial surface, on blood vessels, or freely among axons; white matter astrocytes are usually called fibrous astrocytes (Butt and Ransom, 1989).

C. Function of astrocytes

1. Ion Homeostasis

Homeostatic control of $[K^+]_o$ is needed because brain $[K^+]_o$ can influence transmitter release (Balestrino et al., 1986), cerebral blood flow (Kontos, 1981), ECS volume (Dietzel et al., 1980; Ransom et al., 1985), glucose metabolism (Salem et al., 1975), and neuronal activity (Baylor and Nicholls, 1969). One of the best-established functions of astrocytes is regulation of brain $[K^+]_o$.

Neural activity can rapidly increase $[K^+]_o$ which is tightly regulated to a resting level of about 3 mM (Ransom and Carlini, 1986). The increase in $[K^+]_o$ is proportional to the intensity of neural activity but has a so-called “ceiling” level of accumulation of 10 to 12 mM (Connors et al., 1982), which is only exceeded under pathological condition (Hansen, 1985). If diffusion alone were responsible for dissipating K^+ released from neurons, it is easily calculated that extracellular K^+ accumulation would exceed 10 mM during normal neural activity, whereas measured increases in $[K^+]_o$ are in the range of 1 to 3 mM indicating powerful control mechanisms (Somjen, 1979).

K^+ released by firing neurons is actively accumulated by astrocytes through three pathways. The sodium pump and an anion transporter both take up K^+ ; the sodium pump relies directly on the availability of ATP, whereas the anion transporter is indirectly powered by the energy stored in the transmembrane Na^+ gradient. The presence of channels for Cl^- and K^+ , allow Donnan forces to produce KCl influx, these mechanisms along with K^+ spatial buffering, prevent $[K^+]_o$ from exceeding ~12 mM. Increases in $[K^+]_i$ are seen during neural activity as $[K^+]_o$ increases (Newman, 1995; Ransom et al., 2000; Orkand, 1986).

The idea that focal increases in $[K^+]_o$ could be redistributed by glial cells was introduced by Kuffler and colleagues (Orkand et al., 1966). They realized that the selective K^+ permeability of glia coupled with their low-resistance intercellular connections (mediated by gap junctions), would permit them to transport K^+ from focal areas of high $[K^+]_o$, where a portion of the glial network would have a near normal membrane potential (Orkand et al., 1966).

As it pertains to Kuffler's initial discovery, the search for the K⁺ channel(s) responsible for the large resting K⁺ conductance in astrocytes and hence the channel underlying spatial buffering has recently come to closure. Most researchers now believe that Kir4.1 (KCNJ10), an inwardly rectifying K⁺ channel, is largely responsible for establishing and maintaining the glial resting membrane potential, and indeed appears, at least, partially, responsible for transmembrane K⁺ fluxes in spatial buffering (Olsen and Sontheimer, 2008).

2. Transmitter Removal

Removal of neurotransmitters especially glutamate in the synaptic cleft is one of the major functions of astrocytes. Glutamate is a potent neurotoxin and has been implicated in stroke, amyotrophic lateral sclerosis and epilepsy (Anderson and Swanson, 2000). Highly efficient glutamate transporters remove synaptically released glutamate and also keep the extracellular concentration of this amino acid at about 2 μM (Benveniste et al., 1984). Glutamate transporters are expressed in oligodendrocytes, neurons, microglia, and astrocytes, but transporters in astrocytes are quantitatively the most important in regulating glutamate concentration at synapses and in the extracellular space (Anderson et al., 2000).

Five main types of glutamate transporters have been described: GLAST (EAAT 1), GLT-1 (EAAT 2), EAAC 1 (EAAT 3), EAAT 4, and EAAT 5 (Anderson et al., 2000). EAAC 1 / EAAT 4 transporters are neuronal, mostly localized on the cell body and dendrites (Anderson et al., 2000), whereas GLAST, which is more heavily expressed in the cerebellum, and GLT-1, which is more

prevalent in the forebrain, are predominantly glial (Rothstein et al., 1994). Finally, EAAT5 is only found in the retina where it is principally localized to photoreceptors and bipolar neurons in the retina (Pow and Barnett, 2000). Glutamate uptake into astrocytes is driven by the electro-chemical gradients of Na^+ and K^+ , with a stoichiometry of 3 Na^+ and 1 H^+ in, and 1 K^+ out with the uptake of each glutamate anion (Anderson et al., 2000; Rose and Ransom, 1998). The resulting increase in $[\text{Na}^+]_i$ must be corrected by a cycle of the Na^+ pump and ATP consumption (Deitmer and Schneider, 2000)

Astrocyte membrane facing a glutamate synapse expresses higher levels of GLAST than membrane facing other structures such as pia mater or capillaries (Chaudhry et al., 1995). Most of the glutamate released at synapses appears to be taken up by the adjacent astrocytes (Bergles and Jahr, 1998). The impact of astrocytic glutamate uptake at synapses is most emphatically detected when uptake is blocked. This increases both the amplitude and the duration of the excitatory postsynaptic current (Tong and Jahr, 1994).

3. Metabolic Coupling with Neurons

Astrocyte end-feet surround virtually all brain capillaries, whereas other astrocytic processes ensheath synaptic contacts (Peters et al., 1991; Rohlmann and Wolff, 1996). In addition, astrocytes possess receptors and reuptake sites for a variety of neurotransmitters, including the excitatory neurotransmitter glutamate (Murphy, 1993), whereas astrocytic end-feet are enriched in the specific glucose transporter GLUT-1 (Morgello et al., 1995). Thus astrocytes possess the necessary

features to sense synaptic activity, through receptors and reuptake sites for neurotransmitters, and to couple it with the entry of glucose into the brain parenchyma (Tsacopoulos and Magistretti, 1996).

At glutamatergic synapses, presynaptically released glutamate is terminated by an efficient glutamate uptake system located primarily in astrocytes. Glutamate is cotransported with Na^+ , resulting in an increase in the intra-astrocytic concentration of Na^+ , leading to an activation of the astrocyte Na^+/K^+ ATPase. Activation of the Na^+/K^+ ATPase stimulates glycolysis (i.e., glucose utilization and lactate production). Lactate, once released by astrocytes, can be taken up by neurons and serve them as an adequate energy supply (Magistretti et al., 1999).

The release of glutamate from synaptically active neurons stimulates glucose uptake in nearby astrocytes. The extent of glucose uptake would be proportional to the extent of activity, thereby “coupling” neuronal activity to glucose utilization (Pellerin and Magistretti, 1994).

Another facet of neuron-glia metabolic interactions concerns glycogen. Glycogen, the storage form of glucose, is the largest energy reserve in the brain and it is almost exclusively localized in astrocytes. The levels of glycogen appear to vary in register with synaptic activity and are tightly regulated by a variety of neurotransmitters (Magistretti et al., 1993). Recent results indicate that astrocytic glycogen in the white matter is readily available to axons, mainly as lactate, and sustains their function during glucose withdrawal (Wender et al., 2000).

Blood glucose first encounters astrocytic end-feet as it is transported into the brain. In the absence of glucose, astrocytic glycogen is broken down to lactate,

which is transported to the extracellular space via a monocarboxylate transporter (MCT). It is then taken up by an MCT in axons and is oxidatively metabolized to produce energy needed to sustain excitability. LDH5 preferentially reduces pyruvate to lactate, whereas LDH1 preferentially oxidizes lactate to pyruvate. Neurotransmitters such as norepinephrine, vasoactive intestinal peptide, and adenosine, promote glycogenolysis (Sorg and Magistretti, 1992). These emphasize that astrocytes can subsist, at least transiently, on glycolytic energy metabolism, whereas axons require oxidative metabolism.

D. Purinergic receptors expressed in astrocytes

Purinergic receptors are divided into two groups; ionotropic receptors (P2X) and metabotropic receptors (P2Y). P2X receptors have now been demonstrated in cultured astrocytes, notably the P2X₇ receptor, which increases intracellular calcium levels and causes purine release (Ballerini et al., 1996). There is also direct immunohistochemical evidence for glial expression of P2X₁ (Loesch et al., 1998) and P2X₂ (Kanjhan et al., 1999) subtypes, and hippocampal astrocytes have been shown to co-express P2X₁₋₄, P2X₆ and P2X₇ subunits (Kukley et al., 2001). The evidence for P2Y expression in cultured astrocytes came from the hippocampus (Bernstein et al., 1998), and a study showing that single cerebellar astrocytes express P2Y₁ receptors, plus either P2Y₂ or P2Y₄, with 30~40% also expressing the P2Y₆ receptors (Jimenez et al., 2000). Immunohistochemical confirmation of P2Y₁ expression by astrocytes have been demonstrated

specifically in white matter areas such as corpus callosum, medullary tracts and optic nerve (Moran-Jimenez and Matute, 2000). In addition, Zhu and Kimelberg (2001) provided evidence of a marked up-regulation of mRNA for P2Y₂ receptors during astrocyte development, whereas mRNA for P2Y₁ receptors was present at all ages.

E. Glutamate receptors expressed in astrocytes

Astrocyte responses to glutamate were first observed in cultured astroglia isolated from neonatal animals (Bowman and Kimelberg, 1984; Kettenmann et al., 1984; Kettenmann and Schachner, 1985). Astrocytes have been studied within brain slices or shortly after dissociated with culturing these cells. These studies demonstrated that noncultured immature hippocampal astrocytes possess functional metabotropic, AMPA and possibly NMDA glutamate receptor subtypes (Porter and McCarthy, 1997; Steinhäuser and Gallo, 1996).

There are eight different subtypes (mGlu1-8) of metabotropic glutamate (mGlu) receptors and three sub-grouping based on agonist pharmacology, coupling to specific signal transduction pathways, and sequence homology (Pin and Duvoisin, 1995). The expression of mGlu receptors in glial cells was subsequently investigated by reverse transcription polymerase chain reaction (RT-PCR), immunohistochemistry, and immunoblotting. In general, most of the reports showed the presence of mGlu3 and mGlu5 receptors in astrocytes, whereas a few studies suggest the presence of other receptor subtypes. Both mGlu3 and mGlu5

receptors have been detected by RT-PCR in hippocampal astrocytes acutely isolated from young (Schools and Kimelberg, 1999) and adult rat (Cai et al., 2000). The mGlu4 receptor has been detected in primary cultures of rat and mouse cortical astrocytes by RT-PCR and immunoblotting in some studies (Besong et al., 2002), but not in others (Biber et al., 1999; Ciccarelli et al., 1997)

F. Calcium Waves of astrocytes

The phenomenon of inducible waves of elevated $[Ca^{2+}]_i$ moving through adjacent astrocytes was first reported in tissue culture by Cornell-Bell and associates (Charles, 1998). Their findings set in motion the idea that intercellular Ca^{2+} waves could be a mechanism whereby astrocytes convey information over long distances in the brain. The mechanism of these waves, which move through cells at a rate of 10 to 20 $\mu\text{m}/\text{sec}$, appears to involve the intracellular formation and intercellular transmission of inositol-1, 4, 5-trisphosphate (IP_3), and the release of an extracellular messenger substance such as ATP (Charles, 1998).

The function of intercellular Ca^{2+} waves in astrocytes could be to coordinate the activity of these glial cells. A more intriguing possibility would be that the Ca^{2+} wave could influence neurons in its vicinity. Indeed Ca^{2+} elevation in astrocytes can cause increases in neuronal $[Ca^{2+}]_i$ (Nedergaard, 1994) and induce action potentials in hippocampal neurons (Hassinger et al., 1995; Parpura et al., 1994). However, there is little evidence to suggest that this actually occurs *in situ* or *in vivo* at physiological levels of activity because of difficulty to determine how to

selectively increase Ca^{2+} in a single astrocyte while recording Ca^{2+} responses from surrounding astrocytes. *In vivo* studies have reported that physiological stimuli do not induce intercellular Ca^{2+} waves propagating through large networks of astrocytes, demonstrating that astrocytes behave relatively independently to each other and do not generally function as a broadly interconnected network (Wang et al., 2006; Schummers et al., 2008). Overall, findings in this area suggest that, while intercellular Ca^{2+} waves might occur in certain experimental conditions *in vitro*, *in situ* and *in vivo*, there is little evidence for long-distance signaling between astrocytes under physiological conditions.

G. Gliotransmitters

1. The Concept of Gliotransmission

In general, gliotransmission refers to the process whereby astrocytes release gliotransmitters (i.e., glutamate, ATP, D-serine) to affect synaptic activity (Halassa et al., 2007). Astrocytic release of glutamate and ATP has been most extensively studied. Most recent studies suggest that cultured astrocytes release gliotransmitters via a number of different mechanisms (Kimelberg et al., 2006; Liu et al., 2006; Kang et al., 2008; Stout et al., 2002; Ye et al., 2003; Duan et al., 2003; Fellin et al., 2006; Anderson et al., 2000).

In each of these situations, it is likely that the release mechanism is Ca^{2+} independent and active primarily under pathological conditions. However, it has

been suggested recently that a fraction of astrocytes *in situ* release neuroactive molecules in a Ca^{2+} -dependent manner to affect synaptic transmission via pre- and postsynaptic mechanisms (Bezzi et al., 1998; Fiacco and McCarthy, 2004; Kang et al., 1998; Lee et al., 2007; Mothet et al., 2005; Navarrete and Araque, 2008; Pascual et al., 2005; Pasti et al., 1997; Serrano et al., 2006; Yang et al., 2003). Although the mechanisms underlying Ca^{2+} -dependent gliotransmitter release are currently under investigation and remain controversial (Kang et al., 2008; Parpura et al., 2004), exocytotic vesicular release of gliotransmitters has received considerable attention due to its Ca^{2+} dependency and potential to occur under physiological condition (Parpura et al., 2004). The findings that astrocytes release gliotransmitters imply that astrocytes representing a potential feed-forward excitatory or inhibitory influence on neuronal activity. However, the physiological relevance of these results remain unclear, since Ca^{2+} -dependent gliotransmission and subsequent modulation of neuronal synaptic activity is both controversial and has not yet been demonstrated to occur *in vivo*.

2. Regulation of synaptic activity by astrocytic glutamate release

There are a number of brilliant findings reporting that increases in astrocytic Ca^{2+} lead to either an increase or decrease in glutamate release from Schaffer collateral terminals innervating CA1 pyramidal neurons. Uncaging IP_3 to selectively increase Ca^{2+} in single astrocytes evokes a global intracellular astrocytic Ca^{2+} increase that triggers an increase in the frequency of spontaneous excitatory postsynaptic AMPA currents (sEPSCs) of CA1 neurons (Fiacco and

McCarthy, 2004). Incubation with group I mGluR antagonists blocked the astrocyte-induced increase in AMPA sEPSC frequency, suggesting that astrocytically released glutamate activates mGluRs on neighboring SC presynaptic terminals to elevate presynaptic Ca^{2+} and increase the probability of neurotransmitter release (Fiacco and McCarthy, 2004).

Recently, a pathway behind astrocytic modulation of synapses by showing that ATP-dependent vesicular release of glutamate followed by $[Ca^{2+}]_i$ elevation from astrocyte terminals showed increase of synaptic efficacy through neuronal presynaptic NMDA receptors (Jourdain et al., 2007). Overall, these findings suggest that astrocytic glutamate release activates presynaptic glutamate receptors on a fraction of neighboring synaptic terminals to enhance presynaptic vesicular release of glutamate.

3. Regulation of synaptic activity by astrocytic ATP release

Several groups have reported at this same synapse *in situ* that electrical SC stimulation evokes an increase in Ca^{2+} , triggering the release of ATP that is converted extracellularly into adenosine, which then suppresses glutamate release from presynaptic terminals via the activation of inhibitory presynaptic adenosine receptors (A_1Rs) (Pascual et al., 2005; Serrano et al., 2006). The expression of a dominant-negative mutation of synaptobrevin 2 (dnSNARE) to interfere with the vesicular release of ATP/adenosine from astrocytes resulted in a decrease of the tonic suppression of synaptic transmission by A_1Rs (Pascual et al., 2005). As a consequence, the dynamic range of synaptic transmission was decreased, leading

to an inhibition of LTP *in situ*. There were other reports about vesicular ATP release. When astrocytic Ca^{2+} elevations are evoked by neurotransmitter release, synaptobrevin 2-dependent exocytotic release might apply to ATP release but not to glutamate release (Araque et al., 2000; Zhang et al., 2004; Perea and Araque, 2007).

4. Mechanisms of gliotransmitters release

Various types of organelles have been proposed to underlie exocytosis of gliotransmitters: from synaptic-like microvesicles (SLMVs) (Bezzi et al., 2004; Crippa et al., 2006; Jourdain et al., 2007), to dense-core granules (Coco et al., 2003; Striedinger et al., 2007), to lysosomes (Zhang et al., 2007), and to extra-large organelles with several μm long diameter (Xu et al., 2007). There are other machineries to release gliotransmitters; swelling-induced activation of volume-regulated anion channels (Kimelberg et al., 2006), volume-sensitive outwardly rectifying chloride channels and maxi-anion channels (Liu et al., 2006), connexin hemichannels (Kang et al., 2008; Stout et al., 2002; Ye et al., 2003), pore-forming P2X_7 purinergic receptors (Duan et al., 2003; Fellin et al., 2006), and reversal of glutamate transporters (Anderson et al., 2000). As described above, astrocytes possessed numerous machineries to release gliotransmitters. However, past studies have not taken into account such heterogeneity. In other words, it was impossible to figure out which one is major machinery for releasing gliotransmitters or which astrocytes mainly release gliotransmitters.

5. Spatial-temporal characteristics of ATP and glutamate release in astrocytes

To observe such heterogeneity of gliotransmitters release from astrocytes, the technologies to obtain spatial-temporal information of the release are needed. Exocytosis from astrocytes was observed with a single vesicle imaging method using synaptopHluorin (SpH) as an optical reporter (Bowser and Khakh, 2007). They imaged single SpH-laden vesicles with total internal reflection fluorescence (TIRF) microscopy. Although they could observe vesicular release from astrocytes, there was no way to find out the contents of vesicles. To overcome this problem, Bezzi and colleagues used the chimerical protein vesicular glutamate transporter 1 (VGLUT1)-pHluorin in combination with epifluorescence and TIRF illuminations (Marchaland et al., 2008). Even though it is expected that main contents were glutamate and some quantity of glutamate is released, it is impossible to know whether the glutamate released from this machinery is the sole machinery of there are other main releasing pathway. Overall, their approaches could get the spatial-temporal information of vesicular release from astrocytes, however, the information about the levels of ATP or glutamate was not captured. There was an approach to trace glutamate itself (Innocenti et al., 2000). They observed NADH converted by L-glutamate dehydrogenase as glutamate. However, it was not certain whether NADH and glutamate show the same property of diffusion and life time. In addition, it showed poor resolution to obtain precise spatial-temporal information of glutamate release from astrocytes.

In my experiments, I applied novel ATP and glutamate imaging to astrocytes for the first time. By using these technologies, I succeeded in observing heterogeneity of astrocytes in terms of gliotransmitters release and clarified the spatial-temporal characteristics of ATP and glutamate release from astrocytes.

Thesis Aims

There have been reports that gliotransmitters (i.e. ATP, glutamate, D-serine) released from astrocytes modulate synaptic activities. For examples, astrocytic release of ATP that is converted extracellularly into adenosine suppresses glutamate release from presynaptic terminals via the activation of inhibitory presynaptic adenosine receptors (A_1 Rs) (Pascual et al., 2005; Serrano et al., 2006). On the other hand, many researchers have reported that glutamate released from astrocytes increase the probability of neurotransmitter release from presynaptic terminals and induces extrasynaptic NR2B subtype NMDA-mediated slow inward currents in a population of hippocampal CA1 pyramidal neurons (Angulo et al., 2004; Fellin et al., 2004; Jourdain et al., 2007).

The astrocytic release of gliotransmitters such as ATP and glutamate has been observed in cultured astrocytes by measuring the concentration of gliotransmitter in the extracellular fluid. Although, the fact that astrocytes release gliotransmitters could be confirmed through these methods, dynamics of gliotransmitter release and spatial information cannot be obtained.

Ca^{2+} -dependent gliotransmitter release especially glutamate from astrocytes have been reported by many researchers. Therefore, Ca^{2+} imaging technology which is a brilliant technique to visualize Ca^{2+} mobilization was used to monitor the astrocytic activity to modulate neuronal activity. However, as McCarthy's group has reported for years, there are many evidences that an increase in astrocytic Ca^{2+} is not sufficient to induce glutamate release from astrocytes to

affect neuronal synapses *in situ* (Fiacco and McCarthy, 2004; Fiacco et al., 2007), so that Ca^{2+} imaging is not sufficient for observation of gliotransmitter release.

In this dissertation, I focused on the application of imaging technology to visualize gliotransmitter release from astrocytes. By using imaging technology to monitor ATP and glutamate release from astrocytes, respectively, my study aims at obtaining the first accurate kinetic description of ATP and glutamate release from astrocytes and defining the spatial-temporal characteristics of gliotransmitters release. I believe that it will reveal the physiological significances of gliotransmitter release through the spatial-temporal information.

II. Materials and Methods

A. Solutions and chemicals

The standard Ringer solution contained (mM): 135 NaCl, 5 KCl, 2 CaCl₂, 1 MgCl₂, 5 Na-HEPES, 6 HEPES, and 5 D-glucose (pH 7.4, 290 mosmol/kg-H₂O). Hypotonic bath solution was made by reducing the concentration of NaCl in the standard Ringer solution to 100 mM (210 mosmol/kg-H₂O). Adenosine 5'-diphosphate monopotassium salt (ADP; ≥95%, A5285), adenosine 5'-triphosphate dipotassium salt (ATP; ≥95%, A8937), uridine 5'-triphosphate trisodium salt (UTP: ~97%, U6625), (DL) 2-amino-5-phosphonovaleric acid (AP5; 95%, A6553), 6-methyl-2-(phenylethynyl) pyridine (MPEP; 95%, M5435), Pyridoxal-phosphate-6-azophenyl-2',4'-disulfonic acid tetrasodium salt (PPADS; ≥98%, P178), L-Glutamate dehydrogenase (E.C. 1.4.1.3), nicotinamide adenine dinucleotide (NAD) and its reduced form, NADH were purchased from Sigma-Aldrich, St. Louis, MO. (R, S)-2-chloro-5-hydroxyphenylglycine 2-amino-2-(2-chloro-5-hydroxy-phenyl) acetic acid (CHPG; 95%, 535-62001), 6-cyano-7-nitroquinoxaline-2, 3-dione (CNQX; 98%, 533-26783), adenosine 5'-(gamma-thio) triphosphate (ATP γ S; 80%, 598-00371) was purchased from WAKO Pure Chemical Industries, Ltd. in Osaka, Japan. All reagents were dissolved in Ringer solution. Osmolality of all solutions was measured using a freezing-point depression osmometer (OM802, Vogel, Kevelaer, Germany).

B. Cell preparation

The experimental protocol was approved in advance by the Ethics Review Committee for Animal Experimentation of the National Institute for Physiological Sciences. Astrocytes were obtained from neonatal mouse brain cortex, as previously described (Zhang et al., 2004), with some modifications. The primary culture medium for mouse astrocytes was PC-medium consisting of Eagle's MEM supplemented with L-glutamine 0.292 mg/ml (M0268; Sigma-Aldrich), 100 U/mL penicillin, 0.1 mg/mL streptomycin (Meiji co., Tokyo, Japan), 10% fetal bovine serum (Eqitech-Bio. Inc., Kerrville, Texas, USA), and 2.2 g/L NaHCO₃. Astrocytes were obtained from 1-day old C57/BL6J mouse pups (Charles River Laboratories Japan Inc., Yokohama, Japan). Briefly, the brains of pups were dissected from the skulls, and the cerebellum, olfactory bulbs and meninges were removed. The remaining cerebral cortex was first washed in ice-cold phosphate-buffered saline (PBS) and minced in ice-cold Leibovitz's L-15 medium (Life Technologies, Rockville, MD). The tissue was then dissociated in papain (10 U/mL: Worthington Biochemical Corporation, Lakewood, NJ) dissolved in Earle's balanced salt solution (Invitrogen, Karlsruhe, Germany) for 20 min at 37 °C. The supernatant was removed and resuspended in fresh PC-medium and then cells were triturated by fire-polished pasteur pipette. The cells were passed through a 70 µm nylon filter, plated in culture flasks (Iwaki, Scitech DIV., Ashahi techno glass, Japan) at a density of approximately 2.5×10^5 cells/cm² and cultured in a humidified 5% CO₂ environment. After 12 h ~ 24 h, the medium was replaced,

and cells were subsequently fed every 2 or 3 days with new PC-medium. After becoming confluent, the cells were shaken briefly to remove the microglia growing on the surface of the astrocytes. The cells were then trypsinized (0.25% trypsin (15090; Invitrogen), 0.02% EDTA (E-5134; Sigma-Aldrich)) and transferred to polyethyleneimine (PEI) (P-3143; Sigma-Aldrich,) coated (0.1µg/mL) coverslips (3x10 mm; Matsunami Glass IND. LTD., Osaka, Japan) for the observation. Immunohistochemical tests showed that approx. 93% of the cultured cells were positive for anti-GFAP (glial fibrillary acidic protein) antibody (Z0334, Dako, Carpinteria, CA, USA).

C. Perfusing chamber for measuring extracellular ATP and glutamate concentration released from astrocytes

Small perfusing chamber could exchange solutions for application to astrocytes and collect extracellular fluid of the chamber by every minute. The total volume of the chamber was 200 µL and speed of flow was 200 µL/min. The cells were cultured to confluence on PEI coated (0.1µg/mL) coverslips (3 x 10 mm) for time-course experiments. Every stimulator was dissolved in isotonic Ringer solution. The experiment was performed at room temperature (25 °C).

D. Luciferin-luciferase ATP assay

ATP concentration of the collected extracellular fluid was measured by a luciferin-luciferase assay (ATP Luminescence Kit; AF-2L1, DKK-TOA Co., Tokyo, Japan) with an ATP analyzer (Luminescencer – JNR II AB-2300, ATTO Co., Tokyo, Japan), as previously described (Sabirov and Okada, 2005) with modifications. The amount of ATP released by cells can be indirectly calculated by measuring in real time the number of photons produced by cells incubated in the luciferin–luciferase assay with a photomultiplier. The experiment was performed at room temperature (25 °C).

E. Assay of glutamate release

The collected extracellular solutions were measured by the fluorometric glutamate release assay (Liu et al., 2006). The samples were incubated at room temperature for 40 min with 15 µL of 11.2 mg/mL NAD and 1.5 µL of 15 mg/ml L-glutamate dehydrogenase, and the fluorescence of NADH was measured with a MTP-100F fluorometer (Corona electric, Hitachinaka, Japan) using a 340 nm filter and a 410-600 nm filter for excitation and emission, respectively. The relationship between glutamate concentration and NADH fluorescence was tested using 0.1 µM 0.3 µM, 1 µM, 3µM and 10 µM of glutamate dissolved in the standard Ringer solution and was found to be linear over 1 µM. The fluorescence of 3 µM NADH was roughly equal to that observed in the 3 µM glutamate

calibration assay, indicating that the glutamate-dependent NAD conversion to NADH was complete. However, the concentration of extracellular glutamate in samples was below 1 μM , so that it was not able to detect. The experiment was performed at room temperature (25 °C).

F. Visualization of intracellular calcium dynamics in cultured astrocytes

The astrocytes were incubated in the dark for 20 min at room temperature with an acetoxymethylester form of the Ca^{2+} -sensitive fluorescent dye Fluo4-AM (F-23917; Invitrogen) (2 μM) and were washed with warmed standard Ringer solution. The experiment was performed at room temperature. Fluorescence was imaged using CCD camera (NTE/CCD 512 EBFF GR-1. Roper, USA) through a filter set consisting of a 460–480 nm excitation filter, a 485 nm dichroic mirror and a 495–540 nm emission filter. The experiments were performed under an inverted microscope (IX-81; Olympus, Tokyo, Japan). Images were usually acquired at 1 frame /sec and analyzed using MetaFluor (version 7.0; MDS inc., Toronto, Canada), ImageJ software (version 1.4a; NIH). The experiment was performed at room temperature (25 °C).

G. Visualization of ATP dynamics in cultured astrocytes

Released ATP was detected by Luciferin-Luciferase bioluminescence using a mixture of a reagent (Checklite HS set, Kikkoman, Noda-city, Japan) and Ringer solution (4:1 to 1:1). Bioluminescence emitted by the reaction of Luciferin-Luciferase and ATP is detected using an image intensifier (C8600, Hamamatsu Photonics, Hamamatsu, Japan) and a cooled-CCD camera (Cascade 512, Roper, USA) under an upright microscope (BX51WI, Olympus) with x20 water immersion (NA 0.95) or x4 (NA 0.28) dry objective (Furuya et al., 2005, 2008). ATP images (512 x 512 pixels) were acquired each 300 ms or 500 ms and averaged 6 to 10 frames using MetaMorph (version 6.5; MDS inc., Toronto, Canada). The experiment was performed at 30-34°C or sometimes at the room temperature (25 °C).

H. Visualization of glutamate dynamics in cultured astrocytes

Glutamate optic sensor (EOS) was developed by Namiki et al. (Namiki et al., 2007). For biotinylation of astrocytes, the cell culture preparations were treated with 100 µM sulfo-NHS-SS-biotin (21441, Pierce, Rockford, IL, USA) for 30 min at room temperature. Then, biotinylated EOS (1-2 µM) was incubated with 0.83 µM streptavidin for more than 10 min. Fluorescence images of the EOS-immobilized cells were acquired using an inverted microscope (IX-71; Olympus, Tokyo, Japan) equipped with a cooled charge-coupled device (CCD) camera

(Andor Technology, Belfast) and a dry objective ($\times 20$, NA 0.75; Olympus) through a filter set consisting of a 460–480 nm excitation filter, a 485 nm dichroic mirror and a 495–540 nm emission filter. Solution changes during image acquisitions were performed using a puffing system, which allows complete solution exchange within 2 sec, unless otherwise indicated. Image data were analyzed using ImageJ software (version 1.4a; NIH). To obtain ratio images, which represent the relative change in fluorescence (F/F_0) of EOS, each frame was first divided by the averaged pre-stimulating images. The experiment was performed at room temperature (25 °C).

III. Results

A. Extracellular concentration of ATP and glutamate released from astrocytes

Previous experiments measured extracellular ATP and glutamate concentration (Liu et al., 2006; Liu et al., 2008), however, they measured cumulative concentration of extracellular fluid. Therefore, it was impossible to obtain precise time course of ATP and glutamate release because the concentration of these substances would be the balance between the release and the uptake and/or degradation. To trace the release of ATP and glutamate in a time dependent manner, I made a perfusing chamber to collect extracellular fluid during every one minute. Extracellular ATP concentration was measured by the luciferin-luciferase reaction. It has been reported that hypotonic stress elicits astrocytic ATP release (Liu HT et al., 2008), so that hypotonic stress was used as a positive control for astrocytic ATP release. Mechanical stress was also used as a control. As a physiological stimulation, glutamate (1 mM) was applied. By the glutamate stimulation (1 mM), extracellular ATP concentration was increased approximately to the level of 2 nM (Fig. 1A). Glutamate-evoked astrocytic ATP release was delayed compared to the hypotonic stress or mechanical stress. The elevation of extracellular ATP released from astrocytes was observed approximately 10 min after glutamate application.

Extracellular glutamate concentration was measured by the glutamate dehydrogenase method. Unfortunately, glutamate concentration in the extracellular fluid collected during every one minute from the chamber was below the detection level ($>1 \mu\text{M}$) (Fig. 1B). Although there have been reports that hypotonic stress evokes glutamate release from astrocytes (Liu HT et al., 2006), I could not observe the increase of extracellular glutamate levels in my chamber system due to the detection limitation.

B. New technologies to visualize ATP and glutamate release from astrocytes

Although I succeeded in analyzing the time course of ATP as described above, this time resolution (every one minute) was not enough to figure out the physiological relevance of ATP release from astrocytes. In addition, I could not measure the level of extracellular glutamate released from astrocytes in my chamber system. For these reasons, new technology was needed to measure the level of ATP and glutamate. ATP and glutamate imaging were the best solution to obtain the information of ATP and glutamate release from astrocytes with temporal and spatial resolutions. Astrocytic ATP release was visualized by the luciferin-luciferase reaction which was loaded into the extracellular fluid (Fig 2A). Luciferase is the enzyme to make light produced by the oxidation of luciferin (a pigment) in the presence of ATP. The rate of this reaction between luciferin and

oxygen that produces luminescent is extremely fast when they are catalyzed by luciferase, so that it is suitable to visualize ATP release.

To visualize the glutamate release, glutamate optic sensor (EOS) was applied to cultured astrocytes (developed by Namiki et al., 2007). This specific probe for detecting glutamate is a hybrid molecule consisting of glutamate-binding protein (AMPA receptor GluR2 subunit as a glutamate-binding protein) and a small-molecule fluorescent dye (Oregon green). It would be convenient to immobilize the fluorescent probes on the extracellular side of cell membrane to monitor glutamate released from astrocytes. EOS was accordingly anchored onto cell surfaces via a biotin-streptavidin linkage because it is convenient to immobilize the fluorescent probes on the extracellular side of cell membrane (Fig 2B; See materials and methods) (Namiki et al., 2007). When glutamate released from astrocytes binds to this protein, fluorescence intensity is increased.

C. Evaluation of ATP imaging system

To evaluate the ATP imaging system, hypotonic stress-evoked ATP release was observed. A time course of luminescent images of luciferin-luciferase solution loaded-cultured astrocytes was obtained. I detected luminescent signals representing ATP release from astrocytes (Fig 3A, arrowheads). Fig 3B is the one of the examples of astrocytic ATP release (box in Fig. 3A). This representative ATP release showed approximately 120 sec duration for the release time (shown as Fig 3C).

On the other hand, there were some signals which was showing luminescent signal continuously. These signals showed a similar size and shape of cells (Fig. 3A, arrows), so that I hypothesized this phenomenon was an endocytosis of luciferin and luciferase to cells, and ATP inside the cells reacted. To check this hypothesis, apyrase (60 unit/mL), which is the enzyme to degrade ATP immediately, was applied to the extracellular fluid (data not shown). The signals derived from extracellular ATP were supposed to disappear with this enzyme. However, the continuous cell- shaped signals did not disappear although the transient signals were not observable after application of apyrase. Therefore, these cell-shaped and continuous signals were ruled out from the analysis. Interestingly, this endocytosis mainly occurred in microglia. Astrocytes showed these false signals occasionally only when astrocytes released ATP in a large amount (data not shown). Consequently, luciferin-luciferase reaction-mediated ATP imaging provided temporal and spatial information of ATP release from astrocytes.

D. Evaluation of glutamate imaging system

To evaluate the glutamate imaging system, hypotonic stress-evoked glutamate release was observed. I obtained a time course of fluorescence images of the EOS-stained primary astrocyte cultures. Imaging was obtained during hypotonic stress application. Because EOSs were fixed onto the cell membrane of astrocytes, I got clear image of cell shape (Fig. 4A, a). When glutamate binds to EOS, the fluorescent intensity of EOS is increased. However, it was difficult to identify the

spatial response of fluorescent intensity in the original images (Fig. 4A, a). To map the spatial response of EOS quantitatively, I calculated images that represent a fractional increase in the fluorescence (see Materials and methods) (Fig. 4A; b, c, d, e). There were two types of glutamate release from astrocytes induced by hypotonic stress. First, fast and concentrated glutamate release from a restricted area of single astrocyte was observed (Fig. 4A, b, c, arrowheads; B). This type of glutamate release showed rapid responsiveness to hypotonic stress. In other words, in this type, astrocytes released glutamate right after the application of hypotonic stress. In this fast type release, glutamate was released approximately during 10 sec (Fig. 4B and D). Second, I observed another type of glutamate release; slow decay of glutamate release from the entire surface of a single astrocyte (Fig. 4A, d, e arrows; C). It showed slow responsiveness to hypotonic stress and duration of release was about 40 to 50 sec (Fig 4C and D). Consequently, EOS was proven to provide temporally and spatially resolved information as to astrocytic glutamate release.

E. The cell culture condition to observe ATP and glutamate release evoked by physiological stimulation

I successfully introduced ATP and glutamate imaging to cultured astrocytes. To analyze physiological significance of ATP and glutamate release from cultured astrocytes by imaging system, I adjusted the culture condition of astrocytes. My cultured astrocytes had distinctive features; fully confluent culture and passaged

once (for elimination of neurons) before observation (See materials and method). A benefit of this culture condition was an easy collection of data from astrocytes without neuronal influence, so that primary response of astrocytes against stimulation can be analyzed.

F. ATP and glutamate release evoked by physiological stimulation

As described above, I successfully established the ATP and glutamate imaging system. However, these responses were observed under a pathological condition (hypotonic stress). Therefore, it was needed to apply these imaging systems to visualize ATP and glutamate released by physiological stimulations. ATP and glutamate stimulations were mainly concerned as physiological stimulations. First of all, ATP and glutamate release evoked by ATP stimulation were planned to be determined. Although, ATP-evoked glutamate release was successfully observed (Fig. 8), observation of ATP-evoked ATP release had serious problems. Because ATP itself could not be used as a stimulator in the ATP imaging system, I applied other purinergic agonists such as ADP, UTP or adenosine 5'-(gamma-thio) triphosphate (ATP γ S) (data not shown). However, all of these reacted to the luciferin-luciferase system, so that it was impossible to observe ATP-evoked ATP release in my imaging system.

Next, I tried to observe glutamate-evoked ATP or glutamate release using the imaging system. Glutamate-evoked ATP release was successfully observed (Fig. 13). However, in the glutamate imaging system, glutamate, AMPA and NMDA

could not be stimulators because EOS detects these analogs (Namiki et al., 2007). However, metabotropic glutamate receptor subtype 5 agonist, CHPG could be applied (Table 3).

G. Intracellular calcium elevation of astrocytes by ATP stimulation

To analyze the cell response against ATP stimulations, I decided to check the concentration of intracellular calcium in astrocytes after ATP stimulation, because calcium imaging is well established and calcium dependency of glutamate release can be analyzed. I applied Fluo4-AM dye to astrocytes to observe astrocytic intracellular calcium elevation (Fig. 5A). Intracellular calcium elevation of astrocytes was observed with application of low concentration of ATP ($>1 \mu\text{M}$) (Table 1). I measured the change in the intracellular calcium level of every single astrocyte (Fig. 5B). Fig. 5C is the average fluorescent intensity in all astrocytes. By application of ATP ($1 \mu\text{M}$), the intracellular calcium of all astrocytes immediately increased simultaneously. In other words, the peak of intracellular calcium elevation appeared approximately 8 sec after application of ATP stimulation in most (if not all) of the astrocytes. Interestingly, in spite of continuous exposure to the ATP stimulation (100 sec), immediately elevated intracellular calcium levels decreased synchronously approximately after 15 sec (Fig. 5C). Then I counted the ratio of the cell numbers which showed elevated levels of intracellular calcium at every frame (1 sec) (Fig. 5D). By ATP

stimulation, around 100% of astrocytes showed intracellular calcium elevation. Interestingly, 10 μM ATP showed a different pattern of intracellular calcium elevation in astrocytes (Fig. 5E and F). By application of ATP (10 μM), the intracellular calcium level of all astrocytes immediately increased simultaneously as in the case of 1 μM ATP application. Although by 1 μM ATP stimulation, elevated intracellular calcium levels decreased synchronously approximately after 15 sec, 10 μM ATP stimulation maintained intracellular calcium elevation until the removal of stimulation (Fig. 5E and F). Other purinergic receptor agonists were applied to astrocytes. Adenosine diphosphate (ADP), which is an agonist for P2Y₁ and P2Y₁₂ increased intracellular calcium concentration of astrocytes from 1 μM (Table 1; Fig. 5G and H). There was no immediate increase in the intracellular calcium level, but only slow sustained increase was observed (Fig. 5G). However, uridine triphosphate (UTP), a P2Y₂ and P2Y₄ agonist, showed elevated intracellular calcium levels of astrocytes only at 1 mM or higher (Table 1). Consequently, these results suggested that ATP is a potent activator to increase the intracellular calcium levels in astrocytes.

H. Effect of purinergic receptor antagonist on the intracellular calcium levels in astrocytes

To determine purinergic receptors mediating intracellular calcium elevation in astrocytes, I applied purinergic receptors antagonists (suramin and PPADS) together with ATP (Fig. 6, Fig. 7 and Table 2). Suramin (500 μM), which is a

broad antagonist against P2X, P2Y receptor, inhibited increase in intracellular calcium levels and the number of cells that showed elevation of intracellular calcium levels induced by 1 μ M ATP (Fig. 6B). Then, another P2 receptors antagonist, pyridoxal-phosphate-6-azophenyl-2',4'-disulfonic acid (PPADS) was also tested. PPADS acts as a broad P2X receptor antagonist at a low concentration (50 μ M). PPADS (50 μ M) blocked initial increase in the intracellular calcium levels in astrocytes (Fig. 6C) However, at this concentration, PPADS did not inhibit the late phase increase in the intracellular calcium concentration of astrocytes after application of ATP (1 μ M) (Fig. 6C). However, 300 μ M of PPADS, at which concentration both P2X and P2Y receptors are inhibited broadly, blocked both initial and late phase elevation of intracellular calcium levels in astrocytes by ATP (1 μ M) stimulation (Fig. 6D).

Purinergic receptor antagonists (suramin and PPADS) also inhibited an early phase increase in the calcium level elicited by 10 μ M ATP, however, they could not inhibit the late phase intracellular calcium elevation evoked by 10 μ M ATP stimulation (Fig. 7).

I. Analysis of spatial and temporal information of ATP-evoked glutamate release in astrocytes

I applied ATP to astrocytes to observe glutamate release. ATP-evoked glutamate release was observed from 1 μ M ATP (Fig. 8 and Table 3). Plotted data clarified the kinetics and patterns of glutamate release evoked by ATP (1 μ M)

(Fig. 8A). It was revealed that two types of glutamate release existed. Short and concentrated glutamate release from a restricted area of single astrocyte was shown (Fig. 8C). Interestingly, in this releasing type glutamate was released from the edge of cells approximately during 6 sec (Fig 8E). This type of glutamate release was relatively rare compared with the other type; slow type glutamate release. In this type, glutamate was released from the entire surface of a single astrocyte (Fig. 8D). Cells released glutamate during 40~50 sec by this slow type release (Fig. 8F). I confirmed that ATP-evoked glutamate release occurred in GFAP positive astrocytes (Fig. 8B). High concentration (10 μM) of ATP stimulation showed a similar result to 1 μM of concentration (Fig. 9A and B). Other agonists were tested (Table 3). ADP, UTP (>1 μM) and CHPG-evoked (>100 μM) glutamate release from astrocytes.

J. Effect of purinergic receptors antagonists on glutamate release evoked by ATP

To determine purinergic receptors mediating glutamate release in astrocytes, purinergic receptor antagonists (suramin and PPADS) were applied (Table 4). At a concentration which can inhibit P2X and P2Y receptors completely (PPADS 300 μM and suramin 500 μM), ATP-evoked (10 μM) glutamate release was absolutely blocked. At a low concentration of antagonists (PPADS 50 μM and suramin 50 μM) I observed only one astrocyte to release glutamate by ATP stimulation during 4 independent experiments (Fig. 9C and E). In addition,

glutamate released from a restricted area of single astrocyte (Fig. 9D and F). Consequently, it was indicated that ATP-evoked glutamate release in astrocytes through purinergic receptors.

K. Glutamate increased astrocytic intracellular calcium levels only at a high concentration

Next, combining with calcium imaging, glutamate-evoked ATP release was analyzed through the imaging system. First of all, glutamate-evoked intracellular calcium elevation was observed. By the glutamate stimulation, astrocytes showed totally different patterns of intracellular calcium elevation compared with the ATP stimulation. Only by a high concentration of glutamate stimulation (1 mM), astrocytes increased intracellular calcium levels. Also they showed different responsiveness (Fig. 10) compared with ATP stimulation. For example, some astrocytes increased intracellular calcium levels immediately after application of glutamate stimulation but many others increased with a large delay time (Fig. 10A and B). Plotted data of the average fluorescent intensity in all astrocytes (Fig. 10C) revealed that continuous glutamate stimulation maintained the intracellular calcium elevation in astrocytes. Interestingly, by the glutamate stimulation around 20% to 30% of astrocytes increased the intracellular calcium concentration simultaneously, even though all astrocytes eventually showed increased intracellular calcium levels after ATP stimulation (Fig. 10D). Moreover, I counted the number of cells which showed the intracellular calcium elevation more than

once. By glutamate stimulation (1 mM), I observed 92% of astrocytes which showed the intracellular calcium elevation more than once (Table 1), despite approximately 20% to 30% of astrocytes showed increase in the intracellular calcium concentration simultaneously (Fig. 10D). Next, other glutamate receptors agonists were tested. Metabotropic glutamate receptor (mGluR) subtype 5 agonist, 2-chloro-5-hydroxy-phenyl acetic acid (CHPG) (>100 μ M) increased the intracellular calcium levels of astrocytes (Table 1; Fig. 10E and F). These results indicated that high concentration of glutamate was needed to increase the calcium level in our culture condition and that mGluR was involved in this process.

L. Effect of glutamate receptors antagonists to intracellular calcium elevation

To investigate glutamate receptor-mediated intracellular calcium elevation in astrocytes, glutamate receptor antagonists (MPEP, CNQX and AP5) were applied (Table 2). A selective mGluR subtype 5 antagonist, 6-methyl-2-(phenylethynyl) pyridine (MPEP), inhibited the intracellular calcium elevation in astrocytes at 5 μ M (Fig. 11B). The initial phase intracellular calcium elevation, which is 50 sec after application of glutamate, totally disappeared and the late phase intracellular calcium elevation, which is 50 sec and later after initial phase, was also reduced. Higher concentration (50 μ M) of MPEP showed more potent inhibition of intracellular calcium elevation. An AMPA receptor antagonist, 6-cyano-7-nitroquinoxaline-2, 3-dione (CNQX), partially inhibited the increase of the

intracellular calcium in astrocytes at 20 μ M (Fig. 12B). The initial phase intracellular calcium elevation was blocked, however, the late phase was not decreased. A selective NMDA receptor antagonist, 2-amino-5-phosphonovaleric acid (AP5), (50 μ M) could not reduce intracellular calcium elevation of astrocytes by the glutamate stimulation (Fig. 12C). The main machinery of glutamate-evoked intracellular calcium elevation in astrocytes was, therefore, metabotropic glutamate receptor, and minor one, AMPA receptor.

M. Analysis of spatial and temporal information of glutamate-evoked ATP release in astrocytes

On the basis of calcium imaging, glutamate concentration applied to astrocytes was determined to be 1 mM. By the glutamate stimulation (1 mM), the number of the cells releasing ATP was increased (Fig. 13). Every ATP release from astrocytes was plotted in Fig. 13A. I found that only about 1 % (80 out of 6000 cells) of astrocytes released ATP by the glutamate stimulation. Plotted data indicated that ATP release from astrocytes was increased approximately 200 sec after application of glutamate (Fig. 13A). However, because this plotted data possessed too much information, it was difficult to analyze. Therefore, I divided this graph into two parts; amplitude / frequency and the number of astrocytes releasing ATP release (Fig. 13B and C). I took the data of every peak of ATP release from a single cell, and then plotted them (Fig. 13B). This graph indicated that the frequency of ATP release was raised drastically 200 sec after application

of glutamate. Next, I counted the number of peaks per 100 sec (Fig. 13D). It easily demonstrates that the cells that released ATP increased 200 sec after glutamate stimulation. On the other hand, I counted the number of cells releasing ATP at a time point; I defined over 3000 luminescence intensity as positive signal indicating ATP release per each frame (3 sec) (Fig. 13C). Namely, it indicates the cumulative information of releasing duration. There were two types of ATP release from astrocytes based on the releasing duration (Fig. 13E). Short type ATP release showed 30~50 sec of releasing time (Fig. 13E, red line) and the other showed about 200 sec releasing duration (Fig.13E, blue line). Besides, long type ATP release exhibited higher amplitude than the shorter one. After the experiments, I checked which kind of cells released ATP (Fig. 13F). I confirmed glial fibrillary acidic protein (GFAP) positive astrocytes released ATP (Fig. 13F).

N. Effect of glutamate receptor antagonists on ATP release evoked by glutamate

To determine glutamate receptor-mediated ATP release in astrocytes, glutamate receptor antagonists (MPEP, CNQX and AP5) were applied (Fig. 14, 15 and 16). MPEP (50 μ M) drastically blocked the frequency and amplitude of glutamate-evoked astrocytic ATP release (Fig. 14A). Then I counted the number of events of ATP release per 100 sec (Fig. 14C). It was also reduced after the application of glutamate stimulation. In addition, the number of cells releasing ATP was extremely decreased (Fig. 14E). After washing out MPEP, astrocytic ATP release

evoked by glutamate completely recovered (Fig. 14B, D and F). On the other hand, other glutamate receptor antagonists such as CNQX (20 μ M) and AP5 (50 μ M) did not show any inhibitory effect on astrocytic ATP release (Fig. 15 and 16), even though CNQX (20 μ M) inhibited the initial intracellular calcium elevation of astrocytes (Fig. 12B).

These results revealed that glutamate evokes ATP release from astrocytes at 1 mM or higher, and the increase of ATP release was observed approximately 200 sec after application of glutamate. It was suggested that glutamate-evoked ATP release was mediated mainly by metabotropic glutamate receptors.

IV. Discussion

Through my research, ATP or glutamate release from astrocytes was successfully visualized. Astrocytic ATP release was visualized by the luciferin-luciferase reaction which was loaded into the extracellular fluid. Glutamate increased the frequency of the astrocytic ATP release. On the other hand, a novel fluorescent glutamate probe, EOS, which has a good sensitivity and selectivity, provided a portrait of glutamate release from astrocytes for the first time. Also the intracellular calcium elevation in astrocytes was observed. Overall, my research provided the temporal and spatial information of intracellular calcium, ATP-release and glutamate-release in astrocytes, so that I succeeded in analyzing these information collectively. Also both temporal and spatial information of ATP and glutamate release were obtained.

A. The responses of the intracellular calcium elevation in astrocytes which I prepared in my serial experiments

The intracellular calcium elevation of astrocytes by ATP and glutamate stimulation showed extremely different responses; for examples, low concentration of ATP-evoked ($>1 \mu\text{M}$) the intracellular calcium elevation. In contrast, high concentration of glutamate (1 mM or higher) was needed to produce

the elevation of intracellular calcium levels in astrocytes. When it comes to the concentration of glutamate stimulation, it looks too high. A number of experiments used dissociated cell culture to observe the intracellular calcium elevation. They used 1~100 μM of glutamate as a stimulator in their culture system (Cornell-Bell et al., 1990; Pasti et al., 1995; Hua et al., 2004). However, in my culture system, over 1 mM glutamate was needed to evoke the intracellular calcium elevation in all astrocytes. My cultured astrocytes have distinctive features; fully confluent culture and passaged once (for elimination of neurons) before observation (See materials and method). Because cell confluency is an important factor for the cell viability, I only succeeded in observing ATP and glutamate release from astrocytes under the fully confluent culture condition. Another feature of this culture condition was easy collection of data from a single astrocyte without neuronal influence, so that primary response of astrocytes against stimulation can be analyzed. A lot of spatial information obtained through calcium imaging revealed the property of responsiveness in astrocytes for ATP and glutamate stimulation. Interestingly, by ATP stimulation, all astrocytes showed synchronously increased intracellular calcium levels (Fig. 5A), however, glutamate stimulation evoked the intracellular calcium elevation as a group of astrocytes at a distinct time course (Fig. 10A).

B. Pharmacological properties of ATP-evoked astrocytic intracellular calcium elevation

Spatial-temporal information revealed the properties of the intracellular calcium elevation through pharmacological approaches of purinergic receptor agonists and antagonists. ATP is a potent agonist for P2X and P2Y receptors (North and Surprenant, 2000; Kugelgen, 2006). There were huge differences in the intracellular calcium elevation between 1 μ M and 10 μ M ATP. By application of 1 μ M ATP, all astrocytes showed immediately intracellular calcium elevation (Fig. 5C and D) and the peak of intracellular calcium elevation appeared approximately 8 sec after application of ATP (Fig. 5C). Interestingly, in spite of continuous exposure to ATP (100 sec) immediately elevated intracellular calcium levels decreased synchronously approximately 15~25 sec after the peak (Fig 5C). On the other hand, higher concentration (10 μ M) of ATP showed a similar pattern of intracellular calcium elevation at initial phase, however, the elevation of intracellular calcium levels in astrocytes did not disappear during ATP stimulation (Fig. 5E); the late phase intracellular calcium elevation existed despite the level of elevation was decreased compared with initial phase. What caused these different properties by ATP stimulation? I hypothesized the initial response of astrocytes was mediated by P2X receptors, and the late phase was evoked through P2Y receptors. A set of experiments using ADP as a stimulator supported this hypothesis. ADP is a potent P2Y receptor agonist (Kugelgen, 2006) despite it has ability to stimulate P2X receptors at high concentration (>100 μ M) (North and Surprenant, 2000). By 1 μ M ADP, There was no immediate increase in the

intracellular calcium level (the peak was observed approximately 45 sec after the application of ADP), but only slow sustained increase was observed, so that it indicated that the initial response of astrocytes was mediated through P2X receptors. (Fig. 5G).

Pharmacological approaches using purinergic receptor antagonists (suramin and PPADS) supported my hypothesis (Fig. 6 and Fig. 7). By suramin (500 μM) and PPADS (300 μM), the intracellular calcium elevation evoked by ATP (1 μM) was mostly blocked (Fig. 6B and D). At these concentrations, suramin and PPADS inhibit both P2X and P2Y receptors broadly (North and Surprenant, 2000; Kugelgen, 2006). In contrast, 50 μM PPADS (known as a P2X antagonist at this concentration) could not block the late phase intracellular calcium elevation. However, the initial phase was completely inhibited by PPADS (50 μM) (Fig. 6C). On the other hand, blockage of the intracellular calcium elevation evoked by 10 μM ATP showed different patterns (Fig. 7). Suramin and PPADS inhibited the initial intracellular calcium elevation. However, except for the initial phase, the increase of intracellular calcium levels evoked by ATP (10 μM) was not blocked (Fig. 7B, C and D).

C. Property of ATP-evoked glutamate release from astrocytes

Through calcium imaging, I understood the meaning of ATP stimulation to astrocytes. Next, ATP-evoked glutamate release from astrocytes was observed through EOS imaging system. By 1 μM and 10 μM ATP, the glutamate release

from astrocytes was observed (Fig. 8; Fig. 9A and B). Patterns of releasing glutamate release evoked by two concentrations of ATP showed similar patterns regardless of concentration (Fig. 8A and Fig. 9A). Astrocytes started to release glutamate approximately 20 sec after the application of ATP and the peak of release appeared around 30 sec after application. Thus, the data of glutamate release was combined with the information of intracellular calcium elevation (Fig. 17). These figures do not represent simultaneous observation of calcium imaging and glutamate imaging. The representative information from the calcium imaging and glutamate imaging were simply combined with each other. These figures indicate that glutamate was released from astrocytes after the initial intracellular calcium elevation. The delayed glutamate release implies that intra- or inter-cellular events to initiate glutamate release from astrocytes exist. Besides the temporal information, calcium and glutamate imaging technologies provided spatial characteristics between the intracellular calcium elevation and glutamate release. By the ATP stimulation (1 μ M and 10 μ M), all astrocytes showed increased intracellular calcium levels (Fig. 5 and Table 1), however, only about 5% astrocytes released glutamate by the same stimulation (Table 3). Consequently, for the releasing glutamate, other intra- or inter- cellular events are needed besides intracellular calcium elevation.

D. Differences in the dynamics between hypotonic stress-evoked and ATP-evoked glutamate release

Surprisingly, the characteristic of hypotonic stress-evoked glutamate release was different from that of ATP-evoked glutamate release. Glutamate release evoked by hypotonic stress consisted of two components; fast and concentrated glutamate release from a restricted area of single astrocyte (Type I) (Fig. 4A, b, c, arrowheads; B) and slow decay of glutamate release from the entire surface of single astrocyte (Type II) (Fig. 4A, d, e arrows; C). The former (Type I) showed approximately 10 sec release duration and responded synchronously to application of hypotonic stimulation (Fig. 4D, blue line). In contrast, the latter (Type II) was released glutamate approximately during 40 to 50 sec (Fig. 4D, red line). It showed slow responsiveness to application of hypotonic stress. Onset of the latter was delayed around 10 sec after the application when the response of the former had been already finished (Fig. 4D).

On the other hand, I failed to observe “Type I” glutamate release in ATP-evoked glutamate release (Fig. 8). Although short release duration and concentrated glutamate release from a restricted area of single astrocyte was observed (Fig. 8C), it did not respond synchronously to application of ATP stimulation (Fig. 8E). Thus, this is the third type (Type III) release. In addition, the number of “Type III” glutamate was rare. Long type ATP-evoked glutamate release (Fig. 8D and F) showed similar properties to “Type II” in hypotonic stress-evoked glutamate release. Consequently, the big difference between hypotonic

stress-evoked and ATP-evoked glutamate release was the existence of “Type I” glutamate release in the hypotonicity-evoked glutamate release.

“Type I” glutamate release by hypotonic stress and “Type III” glutamate release by ATP stimulation occurred at the edge of astrocytes (Fig. 4B and Fig. 8C). Two possible releasing pathways may exist in this glutamate release from a restricted area at the edge of a single astrocyte (Fig. 18). One is the actual release from a restricted area of cell edges (Fig. 18B). Another is the leakage of glutamate released from the basal side of astrocytes, which contacts to the cover glass (Fig. 18C). The experiment with VGLUT1-pHluorin TIRF illuminations demonstrated vesicular glutamate release from the basal side of astrocytes (Marchaland et al., 2008). In contrast, astrocytes release glutamate from the entire surface of cell body in “Type II” glutamate release (Fig. 4C, Fig. 8D and Fig. 18A).

In addition, the heterogeneity between ATP-evoked and hypotonic stress-evoked glutamate release was observed through the experiments. Hypotonic stress-evoked glutamate release showed strong response (released from approximately 50% of cells) (Fig. 4A). In contrast, as described above, only about 5% astrocytes released glutamate by the ATP stimulation (Table 3). What made this difference? No one knows the answer to this, however, similar observations are previously reported. The slow inward currents (SICs) have been reported to be induced in a 100 % cell population by hypo-osmotic stress in acute slices of hippocampus (Fiacco et al., 2007) and olfactory bulbs (Kozlov et al., 2006). However, there is contrasting results when SICs were measured after stimulating endogenous G_q GPCRs which can increase the intracellular calcium levels in astrocytes; some groups have reported that G_q GPCR agonist application results

in SICs (Angulo et al., 2004; Fellin et al., 2004; Shigetomi et al., 2008), while other groups have failed to record any SICs (Fiacco and McCarthy, 2004; Fiacco et al., 2007; Lee et al., 2007). This discrepancy can be explained by considering the heterogeneity of glutamate release from astrocytes, which has been shown through my experiments.

E. Pharmacological properties of glutamate-evoked astrocytic intracellular calcium elevation

Combination of the calcium imaging and the glutamate imaging analysis provided spatial-temporal characteristics of the responsiveness toward the glutamate stimulation. First of all, pharmacological approaches using glutamate receptor agonists and antagonists were performed through calcium imaging. As described above, ATP is a potent stimulator for increasing the intracellular calcium levels in astrocytes ($>1 \mu\text{M}$) (Fig. 5 and Table 1). However, only by a high concentration of glutamate stimulation (1 mM), astrocytes increased intracellular calcium levels. Also they showed different responsiveness (Fig. 10 and Table 1) compared with the ATP stimulation. Spatial-temporal information of the calcium imaging showed that, by the ATP stimulation, all astrocytes showed synchronously increase in intracellular calcium levels (Fig. 5A), however, glutamate stimulation evoked the intracellular calcium elevation as a group of astrocytes at a distinct time course (Fig. 10A). In other words, by glutamate stimulation (1 mM), I observed 92% of astrocytes which showed the intracellular

calcium elevation more than once (Table 1), despite approximately 20% to 30% of astrocytes showed increase of the intracellular calcium concentration simultaneously (Fig. 10D)

Which kind of glutamate receptors were involved in the increase of intracellular calcium levels in astrocytes by glutamate stimulation? Pharmacological approaches using glutamate receptor antagonists (MPEP for metabotropic glutamate receptor 5; CNQX for AMPA receptor; AP5 for NMDA receptor) were analyzed (Fig. 11 and Fig. 12). By MPEP (5 μ M and 50 μ M), the intracellular calcium elevation evoked by glutamate (1 mM) was drastically inhibited (Fig. 11B and C). Especially, the initial phase (50 sec after the application) intracellular calcium elevation completely disappeared. The late phase intracellular calcium elevation (50 sec after the initial phase) was potently inhibited by MPEP. However, approximately 10 % astrocytes showed increased intracellular calcium levels (left panels of Fig. 11B and C). Higher concentration (50 μ M) of MPEP (Fig. 11C) showed more potent inhibitory effect than that of 5 μ M MPEP (Fig. 11B). On the other hand, blockage of the intracellular calcium elevation by CNQX (20 μ M) appeared only to the initial phase, however, the late phase was not decreased (Fig. 12B). AP5 (50 μ M) could not reduce intracellular calcium elevation of astrocytes by the glutamate stimulation (Fig. 12C). These results indicate that metabotropic glutamate receptor is the main pathway to increase the intracellular calcium levels in astrocytes. Interestingly, CHPG-evoked (>100 μ M) the intracellular calcium elevation and the pattern was similar to that of ADP-evoked (1 μ M) intracellular calcium elevation (Fig. 10E and F). However,

the reason why only a high concentration (1 mM) of glutamate evokes the increase of intracellular calcium levels is not clear.

F. Property of glutamate-evoked ATP release from astrocytes

Glutamate-evoked ATP release from astrocytes was observed through Luciferin-Luciferase imaging system. By 1 mM glutamate (but not by 100 μ M glutamate or less), the number of the cells releasing ATP was increased (Fig. 13). The frequency of ATP release from astrocytes was drastically increased approximately 200 sec after the application of glutamate (Fig. 13A, B and D). On the other hand, I counted the number of cells that released ATP; I defined over 3000 luminescence intensity as positive signal indicating ATP release per each frame (3 sec) (Fig. 13C). This indicates that the frequency and duration of ATP release were increased cumulatively.

To determine glutamate receptor-mediated ATP release in astrocytes, glutamate receptor antagonists (MPEP, CNQX and AP5) were applied (Fig. 14, 15 and 16). MPEP (50 μ M) drastically blocked the frequency and amplitude of glutamate-evoked astrocytic ATP release (Fig. 14A). The number of events of ATP release per 100 sec was reduced after the application of glutamate stimulation (Fig. 14C). In addition, the number of cells that released ATP was extremely decreased (Fig. 14E). On the other hand, other glutamate receptors antagonists such as CNQX (20 μ M) or AP5 (50 μ M) did not inhibit astrocytic ATP release evoked by glutamate stimulation (Fig. 15 and 16), even though CNQX (20 μ M) inhibited the initial

intracellular calcium elevation of astrocytes (Fig. 12B). These results suggested that glutamate-evoked ATP release was mainly mediated through metabotropic glutamate receptors.

Why was the frequency of ATP release increased approximately 200 sec after the application of glutamate? The responses of intracellular calcium levels had been observed during 100 sec application of glutamate in the previous experiment. To this end, I analyzed the intracellular calcium level after glutamate stimulation for longer duration time to match with the time frame of ATP imaging (Fig. 19D and E). This experiment revealed that the peak of intracellular calcium levels was observed approximately 200 sec after the application, and it never returned to the basal level thereafter maintaining the increased level of intracellular calcium up to 1300 sec (Fig. 19D). Surprisingly, the number of cells showing increased intracellular calcium levels reached around 90 % by long exposure to the glutamate stimulation (Fig. 19D). Consequently, it implies that long glutamate stimulation may be necessary to increase the ATP release in astrocytes. Various intracellular and intercellular events should have been taking place.

G. Heterogeneity of ATP and glutamate release in astrocytes

Spatial-temporal information obtained by the imaging systems revealed heterogeneity of ATP and glutamate release in astrocytes. The results from calcium imaging indicated that ATP elevated the intracellular calcium levels of astrocytes from 1 μ M, and glutamate evoked the intracellular calcium elevation in

astrocytes at 1 mM or higher (Table 1). At those concentrations of stimulation, almost all astrocytes (ca. 100%) showed increased intracellular calcium levels. However, by the same concentration of stimulation, only few astrocytes (ca. 1% in ATP release and ca. 5% in glutamate release) released ATP or glutamate (Fig. 13 for ATP release and Table 3 for glutamate release). In other words, by the stimulation astrocytes showed intracellular calcium elevation homogeneously, however, ATP and glutamate release showed heterogeneity under the same conditions. Through the spatial information provided by the ATP and glutamate imaging, the heterogeneity of ATP and glutamate release in astrocytes was revealed for the first time.

H. Release machineries of gliotransmitters

ATP imaging was performed at 30~34°C (See Materials and Method) because I could not observe glutamate-evoked ATP release from astrocytes through the imaging system at room temperature (~24°C) (data now shown). The maximum luminescent intensity of the luciferin-luciferase reaction was observed at about 22.5°C (Ueda et al., 1979; Ueda et al., 1994), so that I ruled out the effect of temperature on the luciferin-luciferase reaction. In the glutamate imaging, dependence of the glutamate release on temperature was not observed (data not shown). These facts indicate that the machineries mainly releasing ATP from astrocytes after glutamate application are dependent on the temperature. Astrocytes possess several machineries releasing gliotransmitters (See

Introduction). In fact, a majority of experiments examining the machineries releasing gliotransmitters have been performed at room temperature ($\sim 24^{\circ}\text{C}$). However, there have been a few reports about temperature dependence of vesicular release in synapses. An accelerated rate of endocytosis at 35°C have been observed (Fernandez-Alfonso and Ryan, 2004), and recently amperometric recordings from PC12 cells showed that the fusion pore rate and spike frequencies depend strongly on temperature (Zhang and Jackson, 2008). In addition, the L-type $\text{Ca}_v1.4$ voltage-gated calcium channel, which plays a central role in tonic vesicular release at photoreceptor ribbon synapses, showed increased activation at 37°C (Peloquin et al., 2008). However, other machineries, for examples, anion channels (Ernest et al., 2005) and connexons (Sakai et al., 2003; Steffens et al., 2008) did not show increased activities even after raising the temperature over 20°C , even though they showed drastic decrease in the activity below 20°C . Consequently, these facts and my observation of ATP imaging imply that vesicular release may be activated at high temperature ($30\sim 37^{\circ}\text{C}$), so that ATP release from astrocytes is mainly mediated by vesicular release. However, long duration of ATP release (over 300 seconds) is difficult to explain by the vesicular release. Moreover, it is hard to conclude that other machineries are not involved in temperature dependent activities due to the lack of information.

I. Further studies on ATP and glutamate imaging

Past studies have been missing the spatial-temporal characteristics of gliotransmitters release. Astrocytes possess a lot of mechanisms to release gliotransmitters (See introduction). Therefore, the information of astrocytic gliotransmitters release is a mixture of contributions by more than one machinery. My results from imaging experiments revealed the heterogeneity of ATP and glutamate release for the first time implying the heterogeneity of releasing machineries. The temporal information of my research determined dynamics of ATP and glutamate release indicating different releasing mechanisms. The presence of heterogeneity in releasing mechanisms was suggested. Although several gliotransmitter release mechanisms have been suggested (See Introduction), no one knows which one is the major player in gliotransmitter release due to the lack of spatial-temporal information. Imaging technologies provide precise spatial-temporal information of ATP and glutamate release, so that mechanisms of gliotransmitter release can be evaluated.

These imaging technologies can be applied to other co-culture system (neuron-astrocyte), slice culture and in vivo. Further researches using imaging technologies can provide the information of the responses of the cell types (neurons, oligodendrocytes, microglia and so on) to ATP and glutamate released from astrocytes.

V. References

Allen JW, Shanker G, Aschner M. (2001) Methylmercury inhibits the in vitro uptake of the glutathione precursor, cystine, in astrocytes, but not in neurons. *Brain Res* 894:131–140

Aguado F, Espinosa-Parrilla JF, Carmona MA, Soriano E. (2002) Neuronal activity regulates correlated network properties of spontaneous calcium transients in astrocytes *in situ*. *J. Neurosci.* 22:9430–9444.

Angulo MC, Kozlov AS, Charpak S, Audinat E. (2004) Glutamate released from glial cells synchronizes neuronal activity in the hippocampus. *J. Neurosci.* 24:6920–6927

Anderson CM, Swanson RA. (2000) Astrocyte glutamate transport: review of properties, regulation, and physiological functions. *Glia* 32:1–14

Balestrino M, Aitken PG, Somjen GG. (1986) The effects of moderate changes of extracellular K^+ and Ca^{2+} on synaptic and neural function in the CA1 region of the hippocampal slice. *Brain Res* 377:229–239

Ballerini P, Rathbone MP, Di Iorio P, Renzetti A, Giuliani P, D'Alimonte I, Trubiani O, Caciagli F, Ciccarelli R. (1996) Rat astroglial P2Z (P2X7) receptors regulate intracellular calcium and purine release. *NeuroReport* 7: 2533–2537

Baylor DA, Nicholls JG. (1969) Changes in extracellular potassium concentration produced by neuronal activity in the central nervous system of the leech. *J Physiol (Lond)* 03:555–569

Bender AS, Reichelt W, Norenberg MD. (2000) Characterization of cystine uptake in cultured astrocytes. *Neurochem Int* 37:269–276

Benveniste H, Drejer J, Schousboe A, Diemer NH. (1984) Elevation of the extracellular concentrations of glutamate and aspartate in rat hippocampus during transient cerebral ischemia monitored by intracerebral microdialysis. *J Neurochem* 43:1369–1374

Bergles DE, Jahr CE. (1998) Glial contribution to glutamate uptake at Schaffer collateral-commissural synapses in the hippocampus. *J Neurosci* 18:7709–7716

Bernstein M, Behnisch T, Balschun D, Reymann KG, Reiser G. (1998) Pharmacological characterisation of metabotropic glutamatergic and purinergic receptors linked to Ca^{2+} signalling in hippocampal astrocytes. *Neuropharmacology* 37:169–178

Besong G, Battaglia G, D’Onofrio M (2002) Activation of group III metabotropic glutamate receptors inhibits the production of RANTES in glial cell cultures. *J Neurosci* 22:5403

Bezzi P, Carmignoto G, Pasti L, Vesce S, Rossi D, Rizzini BL, Pozzan T, Volterra A. (1998) Prostaglandins stimulate calcium-dependent glutamate release in astrocytes. *Nature* 391:281–285

Bezzi P, Gundersen V, Galbete JL, Seifert G, Steinhauser C, Seifert G, Steinhauser C, Pilati E, Volterra A (2004) Astrocytes contain a vesicular compartment that is competent for regulated exocytosis of glutamate. *Nat Neurosci* 7:613– 620

Biber K, Laurie DJ, Berthele A, Sommer B, Tölle TR, Gebicke-Härter PJ, van Calker D, Boddeke HW. (1999) Expression and signaling of group I metabotropic glutamate receptors in astrocytes and microglia. *J Neurochem* 72:1671–1680

Bowman CL, Kimelberg HK. (1984) Excitatory amino acids directly depolarize rat brain astrocytes in primary culture. *Nature* 311:656–659

Bowser DN, Khakh BS. (2007) Two forms of single-vesicle astrocyte exocytosis imaged with total internal reflection fluorescence microscopy. *Proc Natl Acad Sci USA*. 104:4212-7

Butt AM, Ransom BR. (1989) Visualization of oligodendrocytes and astrocytes in the intact rat optic nerve by intracellular injection of Lucifer yellow and horseradish peroxidase. *Glia* 2:470–475

Cai Z, Schools GP, Kimelberg HK (2000) Metabotropic glutamate receptors in acutely isolated hippocampal astrocytes: developmental changes of mGluR5 mRNA and functional expression. *Glia* 29:70–80

Charles A. (1998) Intercellular calcium waves in glia. *Glia* 24:39–49

Chaudhry FA, Lehre KP, van Lookeren Campagne M, Ottersen OP, Danbolt NC, Storm-Mathisen J. (1995) Glutamate transporters in glial plasma membranes: highly differentiated localizations revealed by quantitative ultrastructural immunocytochemistry. *Neuron* 15:711–720

Ciccarelli R, Sureda FX, Casabona G, Di Iorio P, Caruso A, Spinella F, Condorelli DF, Nicoletti F, Caciagli F. (1997) Opposite influence of the

metabotropic glutamate receptor subtypes mGlu3 and -5 on astrocyte proliferation in culture. *Glia* 21:390–398

Coco S, Calegari F, Pravettoni E, Pozzi D, Taverna E, Rosa P, Matteoli M, Verderio C (2003) Storage and release of ATP from astrocytes in culture. *J Biol Chem* 278:1354–1362.

Connors BW, Ransom BR, Kunis DM, Gutnick MJ. (1982) Activity-dependent K⁺ accumulation in the developing rat optic nerve. *Science* 216:1341–1343

Cornell-Bell AH, Finkbeiner SM, Cooper MS, Smith SJ. (1990) Glutamate induces calcium waves in cultured astrocytes: Long-range glial signaling. *Science* 247:470–473

Crippa D, Schenk U, Francolini M, Rosa P, Verderio C, Zonta M, Pozzan T, Matteoli M, Carmignoto G (2006) Synaptobrevin2-expressing vesicles in rat astrocytes: insights into molecular characterization, dynamics and exocytosis. *J Physiol* 570:567–582

Deitmer JW, Schneider HP. (2000) Enhancement of glutamate uptake transport by CO₂/bicarbonate in the leech giant glial cell. *Glia* 30:392–400

Dietzel I, Heinemann U, Hofmeier G, Lux HD. (1980) Transient changes in the size of the extracellular space in the sensorimotor cortex of cats in relation to stimulus-induced changes in potassium concentration. *Exp Brain Res* 40:432–439

Duan S, Anderson CM, Keung EC, Chen Y, Swanson RA. (2003) P2X₇ receptor-mediated release of excitatory amino acids from astrocytes. *J. Neurosci.* 23:1320–1328

Ernest NJ, Weaver AK, Van Duyn LB, Sontheimer HW. (2005) Relative contribution of chloride channels and transporters to regulatory volume decrease in human glioma cells. *Am J Physiol Cell Physiol* 288:1451-1460

Fellin T, Pascual O, Gobbo S, Pozzan T, Haydon PG, Carmignoto G. (2004) Neuronal synchrony mediated by astrocytic glutamate through activation of extrasynaptic NMDA receptors. *Neuron* 43:729–743

Fellin T, Pozzan T, Carmignoto G. (2006) Purinergic receptors mediate two distinct glutamate release pathways in hippocampal astrocytes. *J. Biol. Chem.* 281:4274–4284

Fernandez-Alfonso, T. and Ryan, T.A. (2004) The kinetics of synaptic vesicle pool depletion at CNS synaptic terminals. *Neuron* 41:943–953

Fiacco TA, McCarthy KD (2004) Intracellular astrocyte calcium waves *in situ* increase the frequency of spontaneous AMPA receptor currents in CA1 pyramidal neurons. *J. Neurosci.* 24:722–732

Fiacco TA, Agulhon C, Taves SR, Petracicz J, Casper KB, Dong X, Chen J, McCarthy KD. (2007) Selective stimulation of astrocyte calcium *in situ* does not affect neuronal excitatory synaptic activity. *Neuron* 54:611–626

Fulton BP, Burne JF, Raff MC. (1992) Visualization of O-2A progenitor cells in developing and adult rat optic nerve by quisqualate-stimulated cobalt uptake. *J Neurosci.* 12:4816-33

Furuya K, Akita K, Sokabe M. (2005) Real time imaging of ATP-release in mammary epithelial cells. *Jpn J Physiol* 55:S80

Furuya K, Harada K, Sokabe M. (2008) Three types of ATP-release in mammary epithelial cells revealed by ATP imaging. *Purinergic Signaling Suppl* 5: S91

Halassa MM, Fellin T, Haydon PG (2007) The tripartite synapse: roles for gliotransmission in health and disease. *Trends Mol. Med.* 13: 54–63

Hansen AJ. (1985) Effect of anoxia on ion distribution in the brain. *Physiol Rev* 65:101–148

Hassinger TD, Atkinson PB, Strecker GJ, Whalen LR, Dudek FE, Kossel AH, Kater SB. (1995) Evidence for glutamate-mediated activation of hippocampal neurons by glial calcium waves. *J Neurobiol* 28:159–170

Hua X, Malarkey EB, Sunjara V, Rosenwald SE, Li WH, Parpura V. (2004) Ca²⁺-dependent glutamate release involves two classes of endoplasmic reticulum Ca²⁺ stores in astrocytes. *J Neurosci Res* 76:86–97

Innoceti B, Parpura V, Haydon PG. (2000) Imaging extracellular waves of glutamate during calcium signaling in cultured astrocytes. *J Neurosci* 20:1800–1808

Jimenez AI, Castro E, Communi D, Boeynaems JM, Delicado EG, Miras-Portugal MT. (2000) Coexpression of several types of metabotropic nucleotide receptors in single cerebellar astrocytes. *J Neurochem* 75:2071–2079

Jourdain P, Bergersen LH, Bhaukaurally K, Bezzi P, Santello M, Domercq M, Matute C, Tonello F, Gundersen V, Volterra A. (2007) Glutamate exocytosis from astrocytes controls synaptic strength. *Nat Neurosci* 10:331–9

Kang J, Jiang L, Goldman SA, Nedergaard M. (1998) Astrocyte mediated potentiation of inhibitory synaptic transmission. *Nat. Neurosci.* 1:683–692

Kang J, Kang N, Lovatt D, Torres A, Zhao Z, Lin J, Nedergaard, M. (2008) Connexin 43 hemichannels are permeable to ATP. *J. Neurosci.* 28:4702–4711

Kanjhan R, Housley GD, Burton LD, Christie DL, Kippenberger A, Thorne PR, Luo L, Ryan AF, (1999) Distribution of the P2X2 receptor subunit of the ATP-gated ion channels in the rat central nervous system. *J Comp Neurol* 407:11–32

Kelly JP, Van Essen DC. (1974) Cell structure and function in the visual cortex of the cat. *J Physiol (Lond)* 238:515–547

Kettenmann H, Backus KH, Schachner M. (1984) Aspartate, glutamate and g-aminobutyric acid depolarize cultured astrocytes. *Neurosci Lett* 52:25–29

Kettenmann H, Schachner M. (1985) Pharmacological properties of g-aminobutyric acid-, glutamate-, and aspartate-induced depolarizations in cultured astrocytes. *J Neurosci* 5:3295–3301

Kettenmann H, Ransom BR. (1995) *Neuroglia*. New York, Oxford University Press

Kimelberg HK, Macvicar BA, Sontheimer H. (2006) Anion channels in astrocytes: biophysics, pharmacology, and function. *Glia* 54:747–757

Kontos HA. (1981) Regulation of the cerebral circulation. *Annu Rev Physiol* 43:397–407

Kozlov AS, Angulo MC, Audinat E, Charpak S. (2006) Target cell specific modulation of neuronal activity by astrocytes. *Proc. Natl. Acad. Sci. USA* 103:10058–10063

Kugelgen I. (2006) Pharmacological profiles of cloned mammalian P2Y-receptor subtypes *Pharmacol Ther.* 110:415-432

Kukley M, Barden JA, Steinhauser C, Jabs R. (2001) Distribution of P2X receptors on astrocytes in juvenile rat hippocampus. *Glia* 36:11 –21

Kuffler SW, Nicholls JG. (1966) The physiology of neuroglial cells. *Ergeb Physiol* 57:1–90

Lee CJ, Mannaioni G, Yuan H, Woo DH, Gingrich, M.B., Traynelis, S.F. (2007) Astrocytic control of synaptic NMDA receptors. *J. Physiol.* 581:1057–1081

Liu HT, Tashmukhamedov BA, Inoue H, Okada Y, Sabirov RZ. (2006) Roles of two types of anion channels in glutamate release from mouse astrocytes under ischemic or osmotic stress. *Glia.* 54:343-57

Liu HT, Toychiev AH, Takahashi N, Sabirov RZ, Okada Y. (2008) Maxi-anion channel as a candidate pathway for osmosensitive ATP release from mouse astrocytes in primary culture. *Cell Res.* 18:558-65

Loesch A, Burnstock G. (1998) Electron-immunocytochemical localization of P2X1 receptors in the rat cerebellum. *Cell Tissue Res* 294:253– 260.

Maienschein, V., Marxen, M., Volkhardt, W. & Zimmermann, H. (1999) A plethora of presynaptic proteins associated with ATP-storing organelles in cultured astrocytes. *Glia* 26:233–244

Magistretti PJ, Sorg O, Martin J-L. (1993) Regulation of glycogen metabolism in astrocytes: physiological, pharmacological, and pathological aspects. In: *Astrocytes: pharmacology and function. Academic Press* 243–265

Magistretti PJ, Pellerin L. (1996) Cellular bases of brain energy metabolism and their relevance to functional brain imaging: evidence for a prominent role of astrocytes. *Cereb Cortex* 6:50–61

Magistretti PJ, Pellerin L, Rothman DL, Shulman RG. (1999) Energyon demand. *Science* 283:496–497

Marchaland J, Calì C, Voglmaier SM, Li H, Regazzi R, Edwards RH, Bezzi P. (2008) Fast subplasma membrane Ca²⁺ transients control exo-endocytosis of synaptic-like microvesicles in astrocytes. *J Neurosci.* 28:9122-3

Miller RH, Fulton BP, Raff MC. (1989) A Novel Type of Glial Cell Associated with Nodes of Ranvier in Rat Optic Nerve. *Eur J Neurosci.* 2:172-180

Moran-Jimenez MJ, Matute C. (2000) Immunohistochemical localization of the P2Y₁ purinergic receptor in neurons and glial cells of the central nervous system. *Mol. Brain Res* 78:50– 58

Morgello S, Uson RR, Schwartz EJ, Haber RS. (1995) The human blood brain barrier glucose transporter (GLUT1) is a glucose transporter of gray matter astrocytes. *Glia* 14:43–54

Mothet JP, Pollegioni L, Ouanounou G, Martineau M, Fossier P, Baux G. (2005) Glutamate receptor activation triggers a calcium-dependent and SNARE

protein-dependent release of the gliotransmitter D-serine. *Proc. Natl. Acad. Sci. USA* 102:5606–5611

Murphy S. (1993) *Astrocytes: pharmacology and function*. San Diego: Academic Press

Namiki S, Sakamoto H, Iinuma S, Iino M, Hirose K. (2007) Optical glutamate sensor for spatiotemporal analysis of synaptic transmission. *Eur J Neurosci.* 25:2249-59

Navarrete M, Araque A. (2008) Endocannabinoids mediate neuronastrocyte communication. *Neuron* 57:883–893

Nedergaard M. (1994) Direct signaling from astrocytes to neurons in cultures of mammalian brain cells. *Science* 263:1768–1771

Newman EA (1995) Glial cell regulation of extracellular potassium. *Neuroglia*. New York: Oxford University Press, 717–731

North RA, Surprenant A. (2000) Pharmacology of cloned P2X receptors *Annu Rev Pharmacol Toxicol.* 40:563-580

Olsen ML, Sontheimer H. (2008) Functional implications for Kir4.1 channels in glial biology: from K⁺ buffering to cell differentiation. *J Neurochem* 107:589-601

Orkand RK, Nicholls JG, Kuffler SW. (1966) Effect of nerve impulses on the membrane potential of glial cells in the central nervous system of amphibia. *J Neurophysiol* 29:788–806

Orkand RK. (1986) Glial-interstitial fluid exchange. *Ann NY Acad Sci* 481:269–272

Parpura V, Basarsky TA, Liu F, Jeftinija K, Jeftinija S, Haydon PG. (1994) Glutamate-mediated astrocyte-neuron signalling. *Nature* 369:744–747

Parpura V, Scemes E, Spray DC. (2004) Mechanisms of glutamate release from astrocytes: gap junction “hemichannels”, purinergic receptors and exocytotic release. *Neurochem. Int.* 45:259–264

Pascual O, Casper KB, Kubera C, Zhang J, Revilla-Sanchez R, Sul JY, Takano H, Moss SJ, McCarthy K, Haydon PG. (2005) Astrocytic purinergic signaling coordinates synaptic networks. *Science* 310, 113–116

Pasti L, Pozzan T, Carmignoto G. (1995) Long-lasting changes of calcium oscillations in astrocytes. A new form of glutamate-mediated plasticity. *J Biol Chem* 270:15203–15210

Pasti L, Volterra A, Pozzan T, Carmignoto G. (1997) Intracellular calcium oscillations in astrocytes: A highly plastic, bidirectional form of communication between neurons and astrocytes *in situ*. *J. Neurosci.* 17:7817–7830

Pellerin L, Magistretti PJ. (1994) Glutamate uptake into astrocytes stimulates aerobic glycolysis: a mechanism coupling neuronal activity to glucose utilization. *Proc Natl Acad Sci USA* 91:10625–10629

Peloquin JB, Doering CJ, Rehak R, McRory JE. (2008) Temperature dependence of Cav1.4 calcium channel gating. *Neurosci* 151:1066-1083

Perea G, Araque A. (2007) Astrocytes potentiate transmitter release at single hippocampal synapses. *Science* 317:1083–1086

Peters A, PalaySL, Webster HD. (1991) *The fine structure of the nervous system*. New York, Oxford Press

Pin JP, Duvosin R. (1995) The metabotropic glutamate receptor: structure and functions. *Neuropharmacology* 34:1–26

Porter JT, McCarthy KD. (1997) Astrocytic neurotransmitter receptors in situ and in vivo. *Prog Neurobiol* 51:439–455

Pow DV, Barnett NL. (2000) Developmental expression of excitatory amino acid transporter 5: a photoreceptor and bipolar cell glutamate transporter in rat retina. *Neurosci Lett*. 11:21-4

Ransom BR, Yamate CL, Connors BW. (1985) Activity-dependent shrinkage of extracellular space in rat optic nerve: a developmental study. *J Neurosci* 5:532–535

Ransom BR, Carlini WG. (1986) Electrophysiological properties of astrocytes. In: *Astrocytes: biochemistry, physiology and pharmacology of astrocytes*. Orlando, FL: Academic Press, 1–49

Ransom BR, Sontheimer H. (1992) The neurophysiology of glial cells. *J Clin Neurophysiol* 9:224–251

Ransom BR. (1995) Gap junctions. In: *Neuroglia*. New York: Oxford University Press, 299–318

Ransom CB, Ransom BR, Sontheimer H. (2000) Activity-dependent extracellular K⁺ accumulation in rat optic nerve: the role of glial and axonal Na⁺ pumps. *J Physiol* 522.3:427–442

Rohlmann A, Wolff JR. (1996) Subcellular topography and plasticity of gap junction distribution on astrocytes. In: *Gap junctions in the nervous system*. RG Landes Company, 175–192

Rose CR, Ransom BR. (1998) pH regulation in mammalian glia. In: *pH and brain function*. New York: Wiley-Liss, 253–275

Rothstein JD, Martin L, Levey AI, Dykes-Hoberg M, Jin L, Wu D, Nash N, Kuncl RW. (1994) Localization of neuronal and glial glutamate transporters. *Neuron* 13:713–725

Sabirov RZ, Okada Y (2005) ATP release via anion channels. *Purinergic Signalling* 4:311-28

Sakai R, Elfgang C, Vogel R, Willecke K, Weingart R. (2003) The electrical behavior of rat connexin46 gap junction channels expressed in transfected HeLa cells. *Eur J Physiol* 446:714-727

Salem RD, Hammerschlag R, Brancho H, Orkand RK. (1975) Influence of potassium ions on accumulation and metabolism of (¹⁴C)glucose by glial cells. *Brain Res* 86:499–503

Serrano A, Haddjeri N, Lacaille JC, Robitaille R. (2006) GABAergic network activation of glial cells underlies hippocampal heterosynaptic depression. *J Neurosci*. 26:5370–5382

Schools GP, Kimelberg HK (1999) mGluR3 and mGluR5 are the predominant metabotropic glutamate receptor mRNAs expressed in hippocampal astrocytes acutely isolated from young rats. *J Neurosci Res* 58:533–543

Schummers J, Yu H, Sur M. (2008) Tuned responses of astrocytes and their influence on hemodynamic signals in the visual cortex. *Science* 320:1638–1643

Shanker G, Allen JW, Mutkus LA, Aschner M. (2001) The uptake of cysteine in cultured primary astrocytes and neurons. *Brain Res* 902:156–163

Shigetomi E, Bowser DN, Sofroniew MV, Khakh BS. (2008) Two forms of astrocyte calcium excitability have distinct effects on NMDA receptor-mediated slow inward currents in pyramidal neurons. *J. Neurosci.* 28:6659–6663

Somjen GG. (1979) Extracellular potassium in the mammalian central nervous system. *Annu Rev Physiol* 41:159–177

Sorg O, Magistretti PJ. (1992) Vasoactive intestinal peptide and noradrenaline exert long-term control on glycogen levels in astrocytes: blockade by protein synthesis inhibition. *J Neurosci* 12:4923–4931

Steinhauser C, Gallo V. (1996) News on glutamate receptors in glial cells. *Trends Neurosci* 19:339–345

Steffens M, Gopel F, Ngezahayo A, Zeilinger C, Ernst A, Kolb HA. (2008) Regulation of connesons composed of human connexin26 (hCx26) by temperature. *Biochim Biophys Acta* 1778:1206-1212

Stout CE, Costantin JL, Naus CC, Charles AC. (2002) Intercellular calcium signaling in astrocytes via ATP release through connexin hemichannels. *J Biol Chem* 277:10482–10488

Striedinger K, Meda P, Scemes E (2007) Exocytosis of ATP from astrocyte progenitors modulates spontaneous Ca^{2+} oscillations and cell migration. *Glia* 55:652–662

Taylor AL, Kudlow BA, Marrs KL, Gruenert DC, Guggino WB, Schwiebert EM (1998) Bioluminescence detection of ATP release mechanisms in epithelia. *Am. J. Physiol.* 275:C1391–C1406

Tong G, Jahr CE. (1994) Block of glutamate transporters potentiates postsynaptic excitation. *Neuron* 13:1195–1203

Tsacopoulos M, Magistretti PJ. (1996) Metabolic coupling between glia and neurons. *J Neurosci* 16:877–885

Ueda I, Kamaya H, Eyring H. (1976) Molecular mechanism of inhibition of firefly luminescence by local anesthetics *Proc. Nat. Acad. Sci. USA* 73:481-485

Ueda I, Shinoda F, Kamaya H. (1994) Temperature-dependent effects of high pressure on the bioluminescence of firefly luciferase *Biophys J* 66:2107-2110

Wang X, Lou N, Xu Q, Tian GF, Peng WG, Han X, Kang J, Takano T, Nedergaard M. (2006) Astrocytic Ca^{2+} signaling evoked by sensory stimulation *in vivo*. *Nat Neurosci* 9:816–823

Wender R, Brown AM, Fern R, Swanson RA, Farrell K, Ransom BR. (2000) Astrocytic glycogen influences axon function and survival during glucose deprivation in central white matter. *J Neurosci* 20:6804–6810

Xu J, Peng H, Kang N, Zhao Z, Lin JH, Stanton PK, Kang J (2007) Glutamate-induced exocytosis of glutamate from astrocytes. *J Biol Chem* 282:24185–24197

Yang Y, Ge W, Chen Y, Zhang Z, Shen W, Wu C, Poo M, Duan S. (2003) Contribution of astrocytes to hippocampal long-term potentiation through release of D-serine. *Proc. Natl. Acad. Sci. USA* 100:15194–15199

Ye ZC, Wyeth MS, Baltan-Tekkok S, Ransom BR. (2003) Functional hemichannels in astrocytes: a novel mechanism of glutamate release. *J Neurosci* 23:3588–3596

Zhang Q, Pangrsic T, Kreft M, Krzan M, Li N, Sul JY, Halassa M, Van Bockstaele E, Zorec R, Haydon PG. (2004) Fusion-related release of glutamate from astrocytes. *J Biol Chem* 279:12724–12733

Zhang XD, Morishima S, Ando-Akatsuka Y, Takahashi N, Nabekura T, Inoue H, Shimizu T, Okada Y (2004) Expression of novel isoforms of the CIC-1 chloride channel in astrocytic glial cells *in vitro*. *Glia* 47:46-57

Zhang Z, Chen G, Zhou W, Song A, Xu T, Luo Q, Wang W, Gu XS, Duan S (2007) Regulated ATP release from astrocytes through lysosome exocytosis. *Nat Cell Biol* 9:945–953

Zhang, Z. and Jackson, M.B. (2008) Temperature dependence of fusion kinetics and fusion pores in Ca²⁺-triggered exocytosis from PC12 cells. *J Gen Physiol* 131:117–124

Zhu YZ, Kimelberg HK. (2001) Developmental expression of metabotropic P2Y1 and P2Y2 receptors in freshly isolated astrocytes from rat hippocampus. *J Neurochem* 77:530–541.

Table 1 Number of cells that showed increased level of intracellular calcium by purinergic and glutamate receptor agonists stimulation

Agonist	1μM	10μM	100μM	1mM
ATP	169/169 (100%)	113/113 (100%)	164/165 (99%)	107/107 (100%)
UTP	144/196 (73%)	166/166 (100%)	201/201 (100%)	Not examined
ADP	106/107 (99%)	110/110 (100%)	105/105 (100%)	96/96 (100%)
Glutamate	Not detected	Not detected	Not detected	168/181 (92%)
CHPG	Not detected	Not detected	63/75 (84%)	71/78 (91%)

UTP, ADP: P2Y receptor agonist

CHPG: mGluR5 specific agonist

Table 2 Effect of purinergic and glutamate receptor antagonists to intracellular calcium elevation

	ATP 1μM	ATP 10μM	Glutamate 1mM
None	100% (99%)	100% (100%)	92.8% (25%)
PPADS 50μM	90.4% (*41%)	100% (*65%)	92.1% (58%)
PPADS 300μM	*78.5% (*26%)	92.6% (*41%)	98.5% (54%)
Suramin 500μM	*30.7% (*7%)	100% (*67%)	*63.8% (22%)
MPEP 5μM	Not examined	Not examined	*75.0% (21%)
MPEP 50μM	Not examined	Not examined	*58.3% (12%)
CNQX 20μM	Not examined	Not examined	*79.5% (46%)
CNQX 200μM	Not examined	Not examined	96.0% (32%)
AP5 50μM	Not examined	Not examined	95.5% (43%)
AP5 500μM	Not examined	Not examined	100% (40%)

Proportion of astrocytes that elevated intracellular calcium level after stimulations
 (Maximum proportion of simultaneous intracellular calcium elevation within 1 sec)
 * p<0.01 compared with ATP 1 μ M, ATP 10 μ M and glutamate 1 mM, respectively

Table 3 Glutamate release from astrocytes

Agonist	1μM	10μM	100μM	500μM
ATP	5/165 (3%)	11/165 (7%)	8/155 (5%)	Not examined
ADP	7/204 (3%)	8/198 (4%)	Not examined	Not examined
CHPG	Not examined	Not examined	6/254 (2%)	18/206 (9%)

Table 4 Effect of purinergic receptor antagonists on glutamate release evoked by ATP

ATP 10μM					
None	10/167,	12/175,	13/158,	10/160	(7%)
PPADS 50μM	1/198,	0/210,	0/165,	0/184	
PPADS 300μM	0/159,	0/165,	0/174,	0/155	
Suramin 50μM	1/254,	0/164,	0/142,	0/186	
Suramin 500μM	0/198,	0/215,	0/225,	0/149	

Figure Legends

Fig. 1 Concentrations of extracellular ATP or glutamate released from astrocytes

(A) Extracellular ATP released from astrocytes was measured by luciferin-luciferase method. By glutamate application, hypotonic stress and mechanical stress, astrocytes released ATP. (B) Extracellular glutamate released from astrocytes was measured by the glutamate dehydrogenase method. Concentrations of glutamate released from astrocytes were below the detection level.

Fig.2 New technologies to visualize ATP and glutamate release

(A) ATP released from astrocytes was visualized by luminescence produced by the luciferin-luciferase reaction. (B) For glutamate imaging, glutamate optic sensor (EOS) was developed using the extracellular domain of AMPA receptor. Fluorescent dyes are attached to these specific receptors, so that when glutamate binds to this protein, fluorescent intensity is increased. EOSs were immobilized using biotin-streptavidin to cell membrane.

Fig. 3 Evaluation of ATP imaging

(A) ATP was released from astrocytes by hypotonic stimulation. (B) One example of ATP release visualized by the luciferin-luciferase reaction. Zero time indicates the start of ATP release. (C) Luminescent intensity was plotted. In this example, ATP was continuously released during around 120 sec.

Fig. 4 Evaluation of Glutamate imaging

(A) EOS was immobilized onto membrane of astrocytes. Glutamate was released from astrocytes by hypotonic stimulation (a). To visualize glutamate release, the change in the fluorescent intensity was observed (b, c, d, and e). There were two types of glutamate release from astrocytes. One type showed fast and concentrated release from a restricted area of single astrocyte (b, c). The other showed slow decay of glutamate release from the entire surface of single astrocyte (d, e). (B) One example of fast and concentrated glutamate release from astrocytes. Zero time indicates the start of glutamate release. (C) One example of slow decay of glutamate release from astrocytes. Zero time indicates the start of glutamate release. (D) Plotted data of two types of glutamate release. Fast types released glutamate approximately during 10 sec (blue line). Around 40~50 sec were the releasing time of glutamate from the entire surface of single astrocyte (red line).

Fig. 5 Intracellular calcium elevation of astrocytes by ATP or glutamate stimulation.

(A) Fluorescent imaging of Fluo4-AM. After the application of ATP (1 μ M), intracellular calcium levels in all astrocytes were increased (right picture). (B) Intracellular calcium elevation of every single astrocyte by ATP (1 μ M) stimulation (C) Average of intracellular calcium levels in all the astrocytes after ATP (1 μ M) application. (D) Proportion of the cell numbers that showed intracellular calcium elevation after ATP (1 μ M) stimulation (E) Average of intracellular calcium levels in all the astrocytes after ATP (10 μ M) application. (F) Proportion of cells that showed intracellular calcium elevation after ATP (10 μ M) stimulation (G) Average of intracellular calcium levels in all the astrocytes after ADP (1 μ M) application. (H) Proportion of cells that showed intracellular calcium elevation after ADP (1 μ M) stimulation

Fig. 6 Effect of purinergic receptor antagonists on the intracellular calcium levels in astrocytes evoked by 1 μ M ATP stimulation

(A) Average of intracellular calcium levels in all the astrocytes after ATP (1 μ M) application (Left). Proportion of the cell numbers that showed intracellular calcium elevation after ATP (1 μ M) stimulation (Right). (B) Suramin (500 μ M), which is a broad P2X, P2Y receptors antagonist, inhibited elevation of intracellular calcium levels (Left) and increase in the number of cells that showed

elevated intracellular calcium levels (Right). (C) PPADS (50 μM), which is broad P2X receptors antagonist at low concentration, did not inhibit increase of the late phase intracellular calcium concentration of astrocytes after application of ATP (1 μM), even though, the initial phase intracellular calcium elevation disappeared. (D) However, 300 μM PPADS (broad P2X, P2Y receptors antagonist at high concentration) potently blocked both phase of elevated intracellular calcium levels in astrocytes by ATP stimulation.

(Red line indicates the magnified average of intracellular calcium levels. Smoke color line indicates average of intracellular calcium levels evoked by 1 μM ATP.)

Fig. 7 Effect of purinergic receptor antagonists on the intracellular calcium levels in astrocytes evoked by 10 μM ATP stimulation

(A) Average of intracellular calcium levels in all the astrocytes after ATP (10 μM) application (Left). Proportion of the cell numbers that showed intracellular calcium elevation after ATP (10 μM) stimulation (Right). (B) Suramin (500 μM) inhibited only the initial phase of increased intracellular calcium levels (Left) and the initial phase of increase in the number of cells that showed elevation of intracellular calcium levels (Right). (C) PPADS (50 μM) did not inhibit increase of the late phase intracellular calcium concentration of astrocytes after application of ATP (10 μM), even though, the initial phase intracellular calcium elevation disappeared. (D) PPADS (300 μM) blocked the initial phase of elevation of

intracellular calcium levels in astrocytes by ATP stimulation, however, the late phase was not inhibited.

(Red line indicates the magnified average of intracellular calcium levels. Smoke color line indicates average of intracellular calcium levels evoked by 10 μ M ATP.)

Fig. 8 Imaging analysis of glutamate release from astrocyte evoked by 1 μ M ATP

(A) Plotted data of 1 μ M ATP-evoked glutamate released from every single astrocyte. Two types of glutamate release exist. (B) GFAP⁺ astrocytes (red) released glutamate (Right). Left panel is fluorescent image of EOS. Yellow boxes indicate glutamate release places. (C) Short and concentrated glutamate release from a restricted area of single astrocyte was shown. Yellow dots surround the release site. (D) Long glutamate release from the entire surface of single astrocyte is other pattern of glutamate release. Yellow dots surround the release site. (E) In the fast type glutamate was released from astrocytes during around 6 sec. (F) The cells from (D) released glutamate during 40~50 sec.

Fig. 9 Imaging analysis of glutamate release from astrocytes evoked by 10 μ M ATP

(A) Plotted data of 10 μ M ATP-evoked glutamate released from every single astrocyte. (B) One of the examples of glutamate release evoked ATP (10 μ M) (C)

One observation of glutamate release with the application ATP (10 μ M) and PPADS (50 μ M). Only one glutamate release was observed. (D) Glutamate release from (C) was released from a restricted area at edge of a single astrocyte. A yellow box surrounds the release site. (E) One observation of glutamate release with the application ATP (10 μ M) and suramin (50 μ M). Only one glutamate release was observed. (F) Glutamate release from (E) was released from a restricted area at edge of a single astrocyte. A yellow box surrounds the release site.

Fig. 10 Intracellular calcium elevation of astrocytes by ATP or glutamate stimulation.

(A) Fluorescent imaging of Fluo4-AM. After the application of glutamate (1 mM), intracellular calcium levels in a group of astrocytes were increased at a distinct time course (right pictures). (B) Intracellular calcium elevation of every single astrocyte by glutamate (1 mM) stimulation (C) Average of intracellular calcium levels in all the astrocytes after glutamate (1 mM) application. (D) Proportion of the cell numbers that showed intracellular calcium elevation after glutamate (1 mM) stimulation (E) Average of intracellular calcium levels in all the astrocytes after CHPG (mGluR5 selective agonist) (1 mM) application. (F) Proportion of cells that showed intracellular calcium elevation after CHPG (1 mM) stimulation.

Fig. 11 Effect of glutamate receptor antagonist (MPEP) to intracellular calcium elevation

(A) Average of intracellular calcium levels in all the astrocytes after glutamate (1 mM) application (Left). Proportion of the cell numbers that showed intracellular calcium elevation after glutamate (1 mM) stimulation (Right). (B) MPEP (5 μ M), which is a selective metabotropic glutamate receptor subtype 5 antagonist, diminished glutamate-evoked initial intracellular calcium elevation, and elevation of intracellular calcium levels in late phase was reduced. (C) MPEP (50 μ M) diminished glutamate-evoked initial intracellular calcium elevation, and elevation of intracellular calcium levels in late phase was reduced. Higher concentration of MPEP showed more potent inhibitory effect.

Fig. 12 Effect of glutamate receptor antagonists (CNQX and AP5) to intracellular calcium elevation

(A) Average of intracellular calcium levels in all the astrocytes after glutamate (1 mM) application (Left). Proportion of the cell numbers that showed intracellular calcium elevation after glutamate (1 mM) stimulation (Right). (B) CNQX (20 μ M) (AMPA receptor antagonist) blocked the initial increase of intracellular calcium concentrations ($p < 0.001$), however, the late phase was not decreased. (C) AP5 (50 μ M) (selective NMDA receptor antagonist) could not reduce intracellular calcium elevation of astrocytes by glutamate stimulation.

Fig. 13 Analysis of ATP imaging

(A) Plotted data of glutamate-evoked ATP released from every single astrocyte (B) This graph contains amplitude and frequency of every ATP release of (A). Vertical lines mean amplitude and peak time of ATP release. (C) The number of cells releasing ATP per one frame (3 sec). (D) The frequency of ATP release was increased approximately 200 sec after glutamate applied. The upper numbers mean the ATP release numbers per 100 sec. (E) By the releasing duration (short and long), ATP release patterns can be divided into two types. Short type of ATP release showed 30~50 sec of release (red line). On the Other hand, long type of ATP release was observed during around 200 sec (blue line). (F) GFAP⁺ astrocytes (red) released ATP (Left). Green fluorescent indicates microglia. Yellow lines are astrocytes which released ATP. Right panel is higher magnification of one astrocyte (white box in left panel) which released ATP.

Fig. 14 Effect of metabotropic glutamate receptor antagonist, MPEP on ATP release evoked by glutamate

(A) MPEP (50 μ M) drastically blocked the frequency and amplitude of glutamate-evoked ATP release. (B) After washing out MPEP, glutamate was applied on the same sight. Glutamate-evoked ATP release (frequency and amplitude) was completely recovered. (C) The upper numbers mean the peaks of ATP release per 100 sec. On the application of 50 μ M MPEP, the number of peaks were decrease (D) After washing out, these were recovered. (E, F) The number of cells releasing

ATP per one frame (3 sec) on MPEP and glutamate was completely reduced (E), and after washing out, it was recovered (F).

Fig. 15 Effect of AMPA receptor antagonist, CNQX on ATP release evoked by glutamate

(A) CNQX (20 μ M) did not blocked drastically the frequency and amplitude of glutamate-evoked ATP release. (B) After washing out CNQX, glutamate was applied on the same sight. ATP release (frequency and amplitude) was slightly increased. (C, D) The upper numbers mean the peaks of ATP release per 100 sec. There was no difference between application of glutamate and CNQX mixture (C) and glutamate application after washing out (D). (E, F) The number of cells releasing ATP per one frame (3 sec) on CNQX and glutamate (E) was not different from that after wash out (F).

Fig. 16 Effect of NMDA receptor antagonist, AP5 on ATP release evoked by glutamate

(A) AP5 (50 μ M) did not blocked drastically the frequency and amplitude of glutamate-evoked ATP release. (B) After washing out AP5, glutamate was applied on the same sight. ATP release (frequency and amplitude) was slightly increased. (C, D) The upper numbers mean the peaks of ATP release per 100 sec. There was no difference between application of glutamate and AP5 mixture (C)

and glutamate application after wash out (D). (E, F) The number of cells releasing ATP per one frame (3 sec) on AP5 and glutamate (E) was not different from that after washing out (F).

Fig. 17 Combination analysis of calcium imaging and glutamate imaging evoked by ATP stimulation

(A) Representative glutamate release evoked by 1 μM ATP was delayed approximately 20 sec compared with average of intracellular calcium elevation (B) Representative glutamate release evoked by 10 μM ATP was delayed approximately 20 sec compared with average of intracellular calcium elevation

Fig. 18 Scheme of glutamate release from astrocytes

(A) Glutamate released from the entire surface of single astrocyte (B) Glutamate released from the restricted area of edge in single astrocytes (C) Glutamate leaked from the basal of single astrocyte

Fig. 19 Combination analysis of calcium imaging and ATP imaging evoked by glutamate stimulation

(A) This graph contains amplitude and frequency of every ATP release. Vertical lines mean amplitude and peak time of ATP release. (B) The number of cells releasing ATP per one frame (3 sec). (C) The frequency of ATP release was

increased approximately 200 sec after glutamate applied. The upper numbers mean the ATP release numbers per 100 sec. (D) The elevated intracellular calcium levels in astrocyte by long duration (1300 sec) exposure to the glutamate (1 mM) stimulation (E) Proportion of the cell numbers that showed intracellular calcium elevation after long duration exposure to the glutamate (1 mM) stimulation.

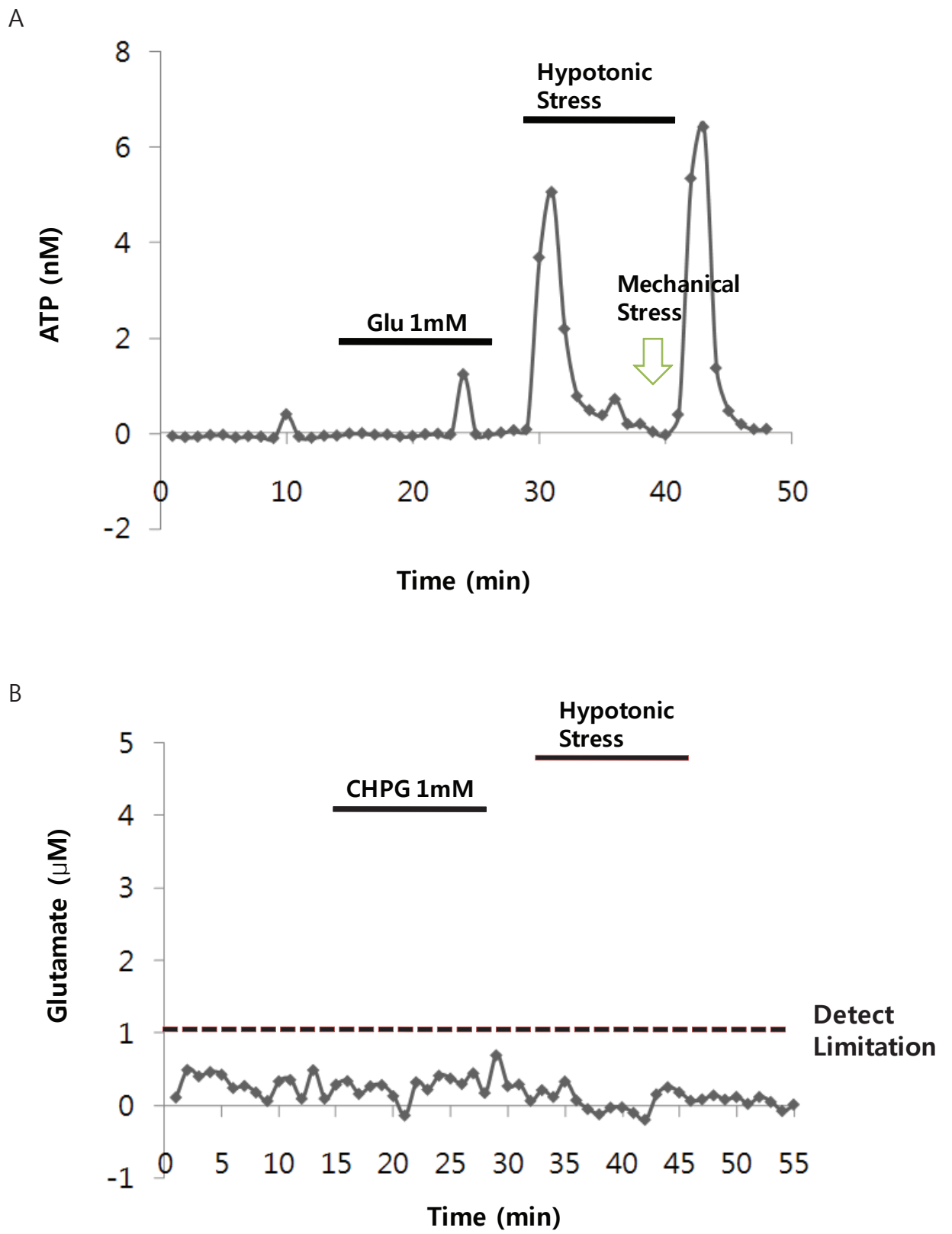
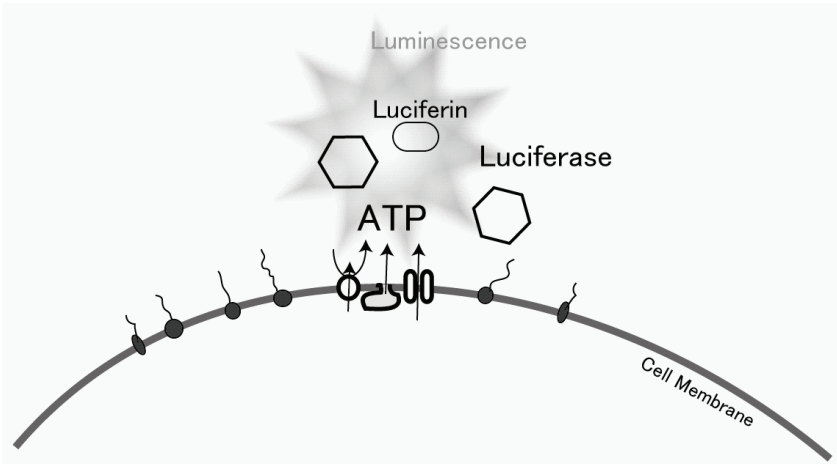


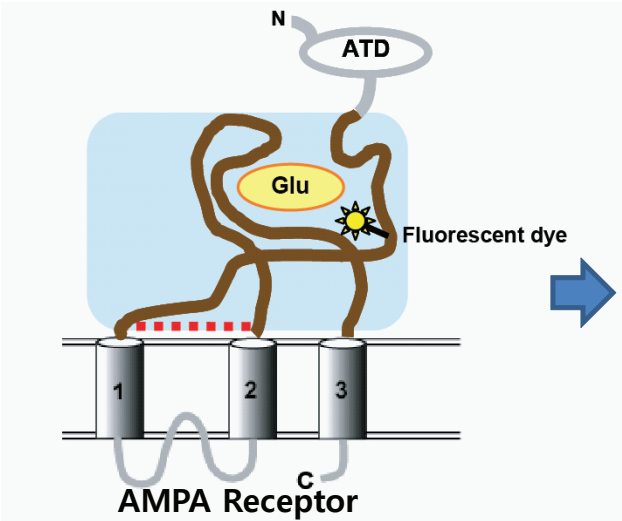
Fig. 1

A. ATP Imaging



B. Glutamate Imaging

Molecular design



Immobilization of EOS

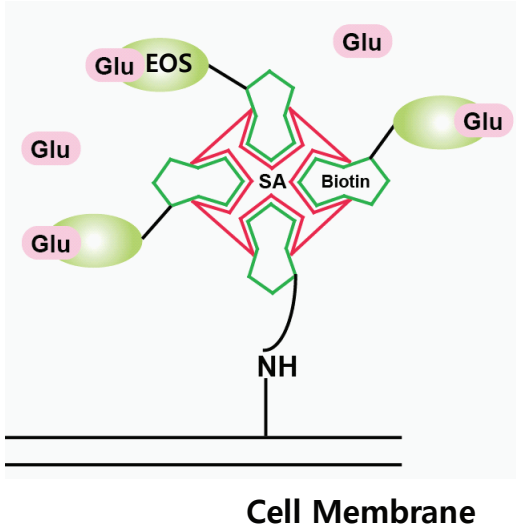
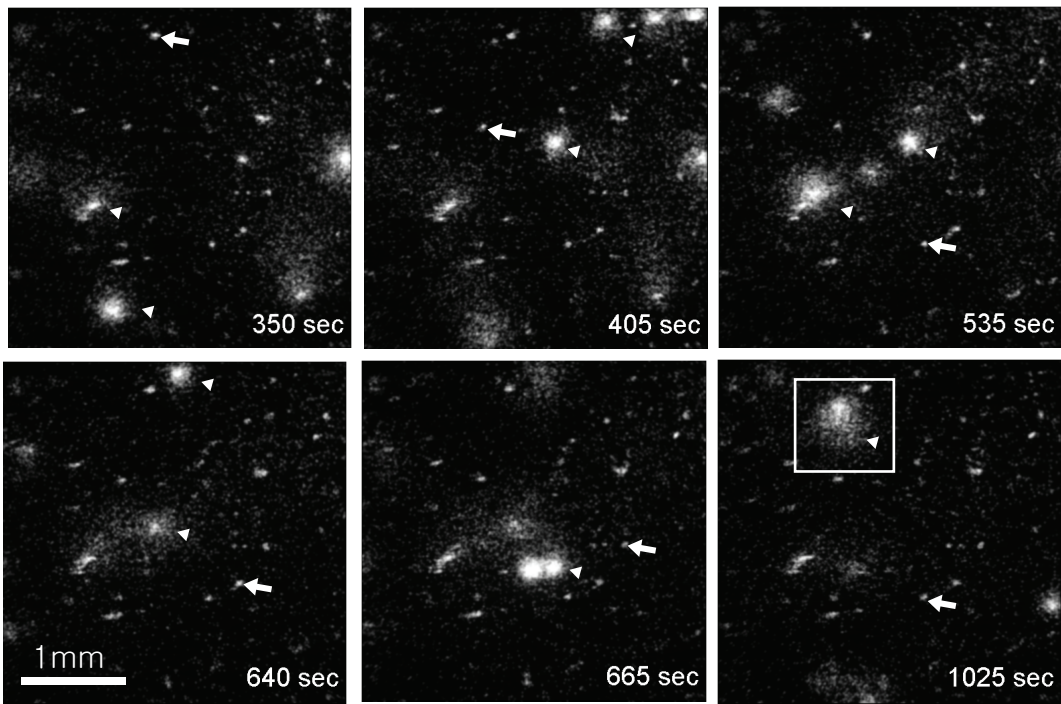
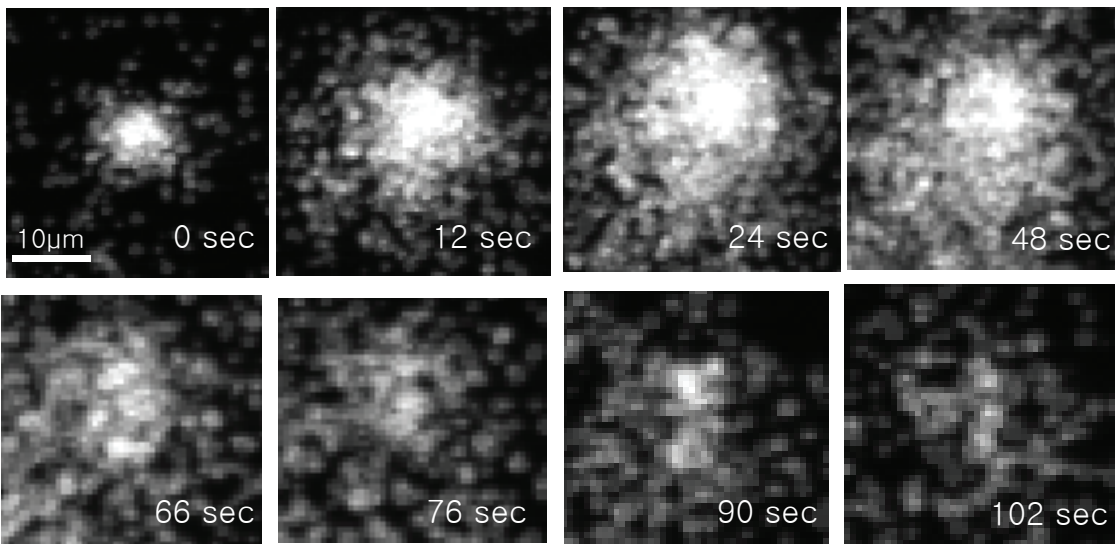


Fig. 2

A



B



C

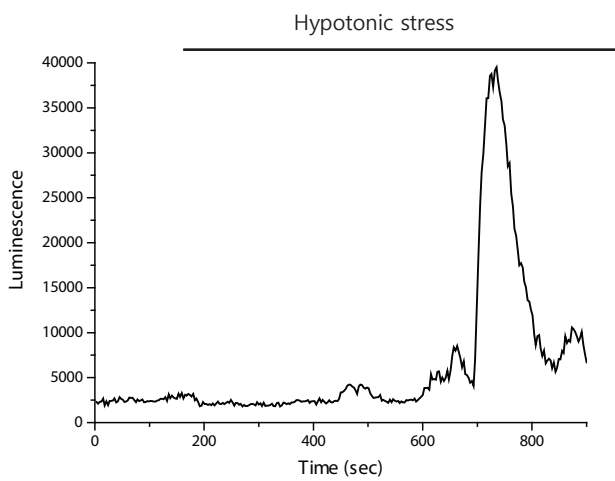


Fig.3

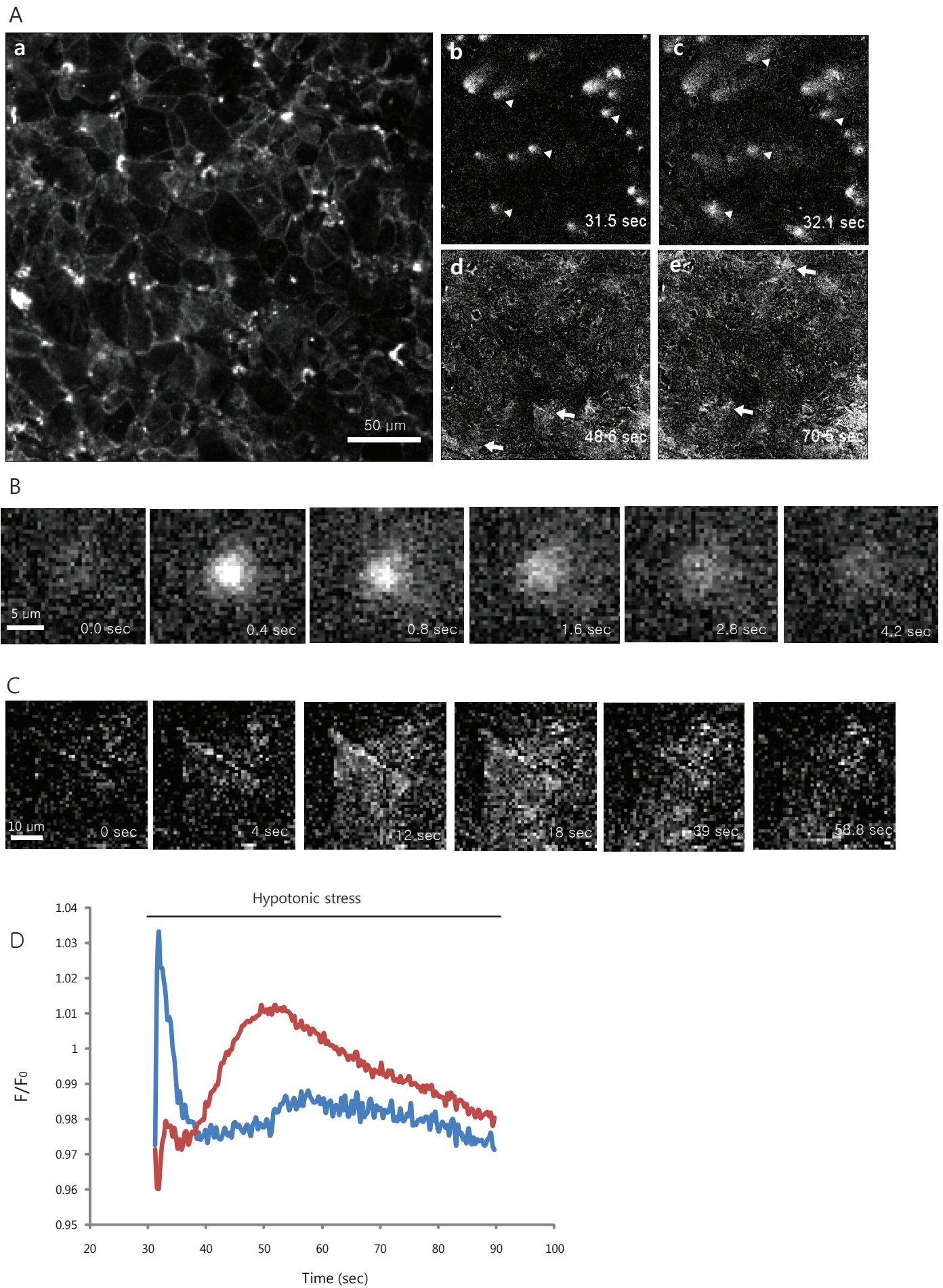


Fig. 4

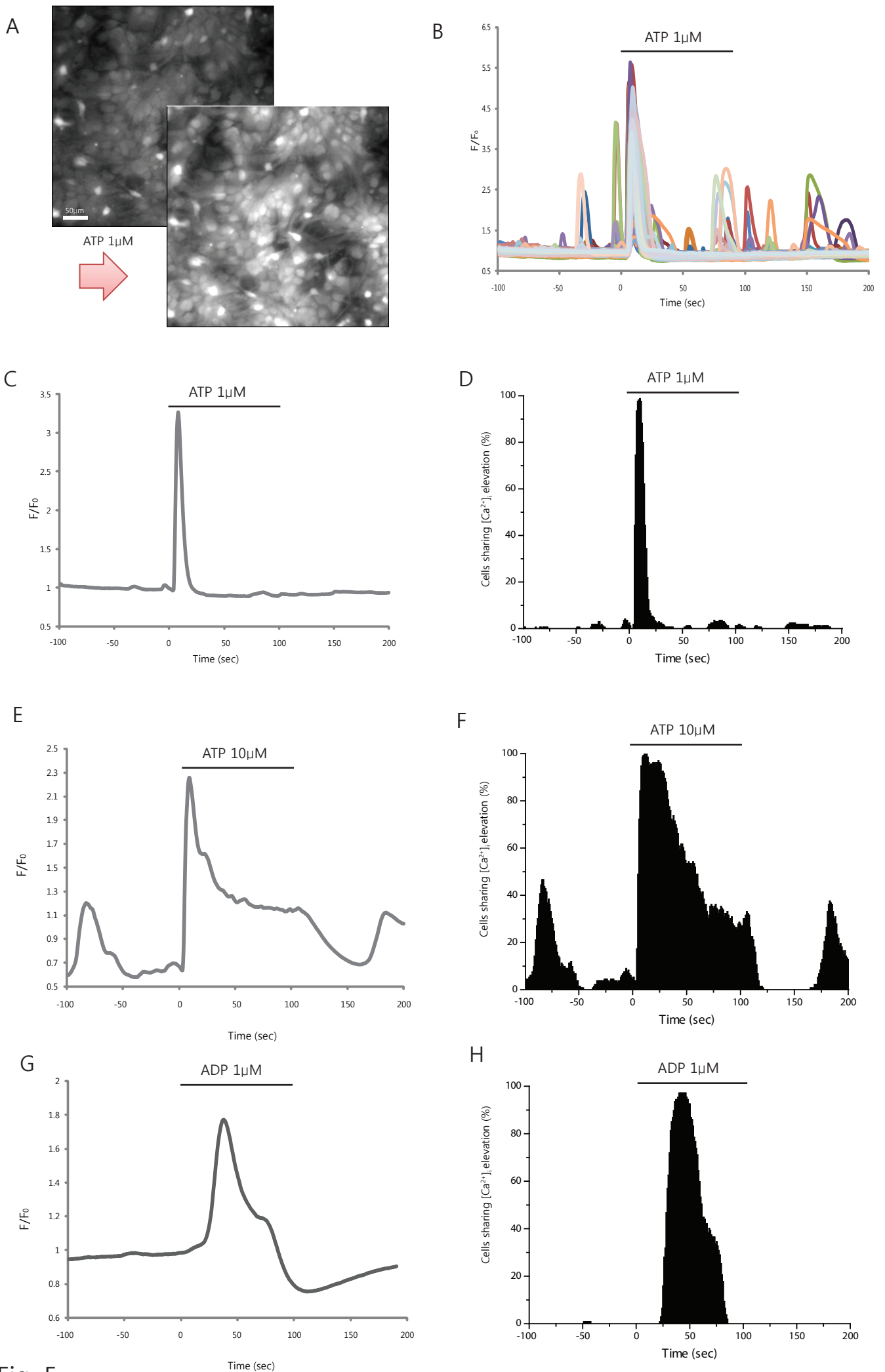


Fig. 5

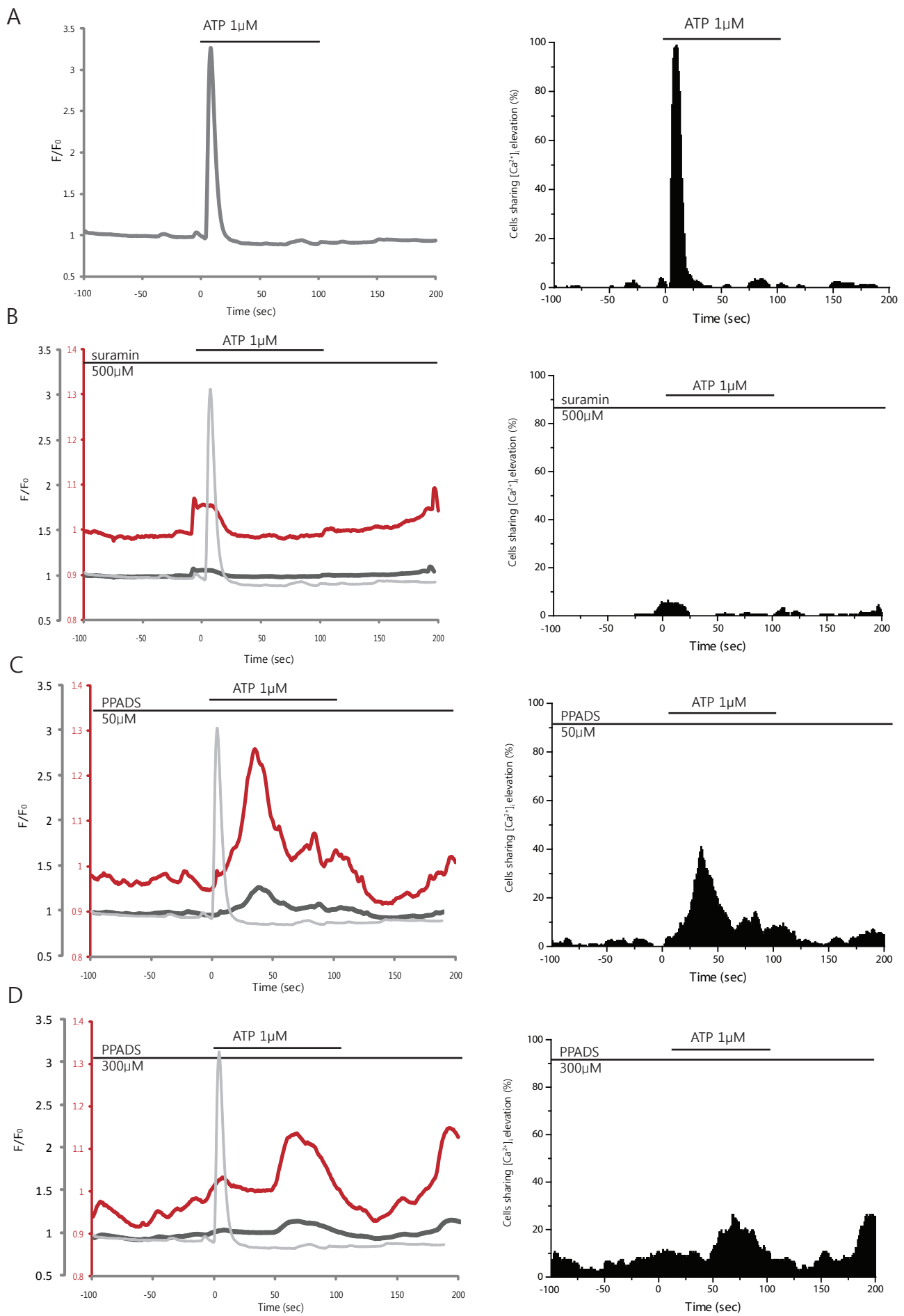


Fig. 6

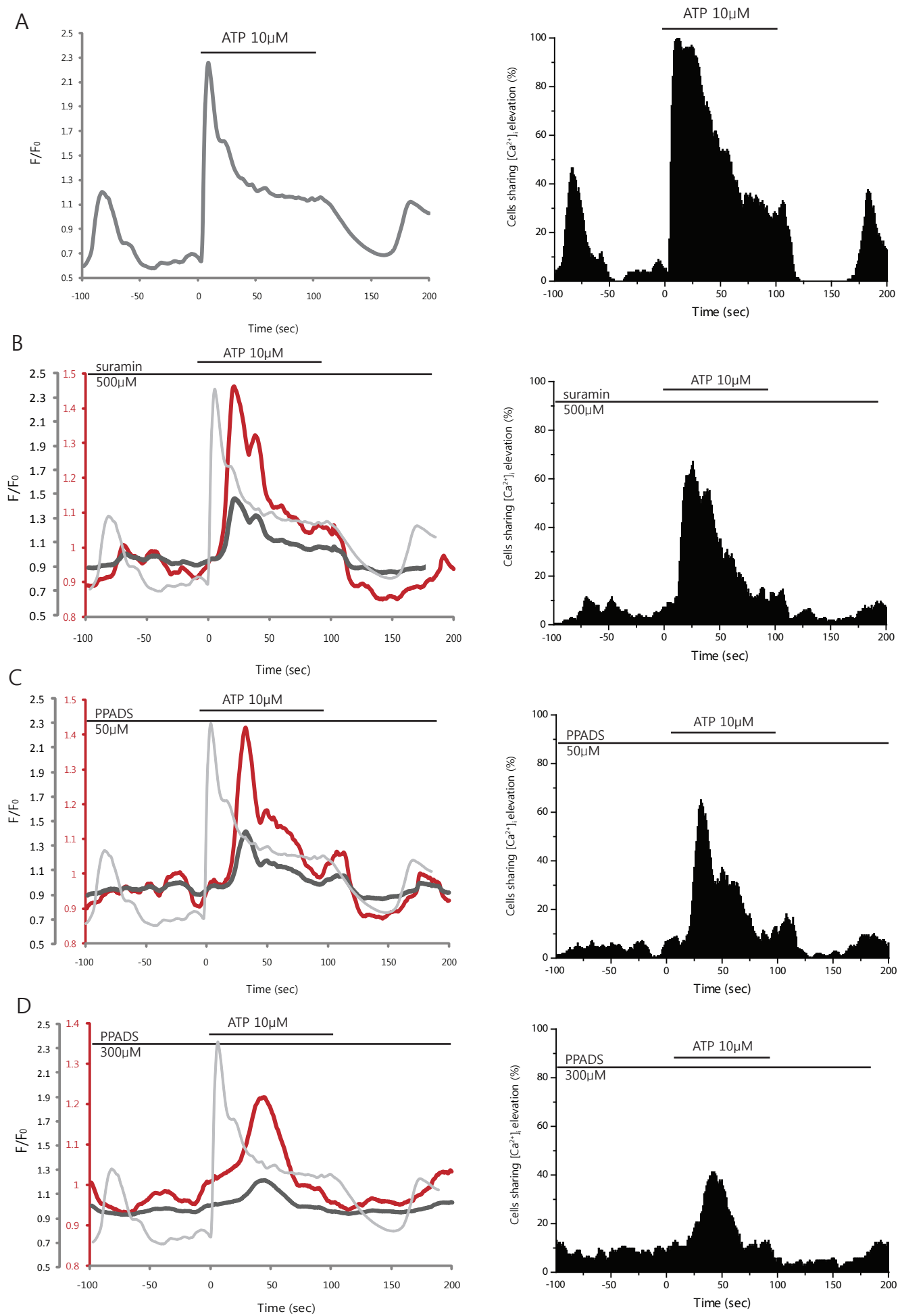


Fig. 7

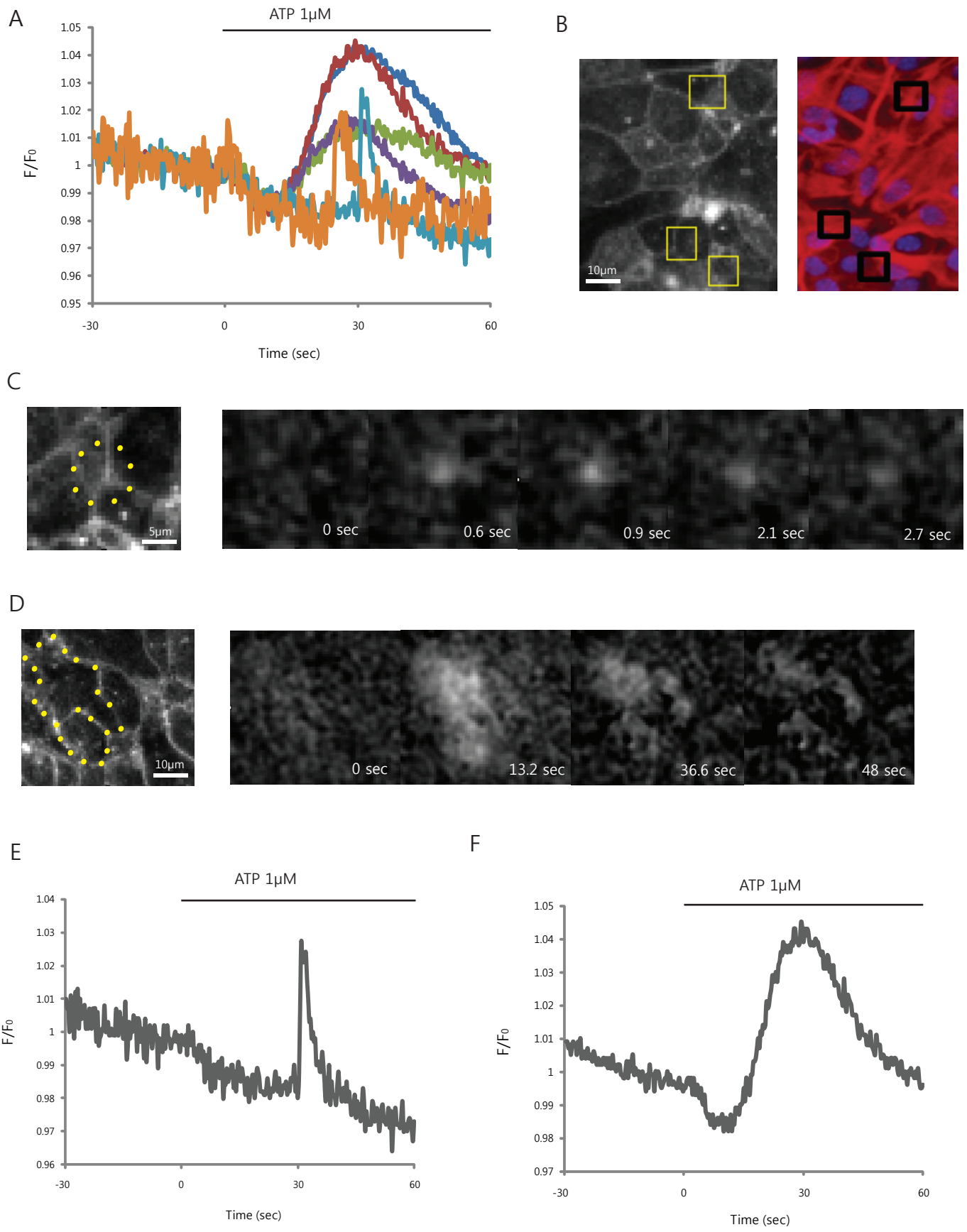


Fig. 8

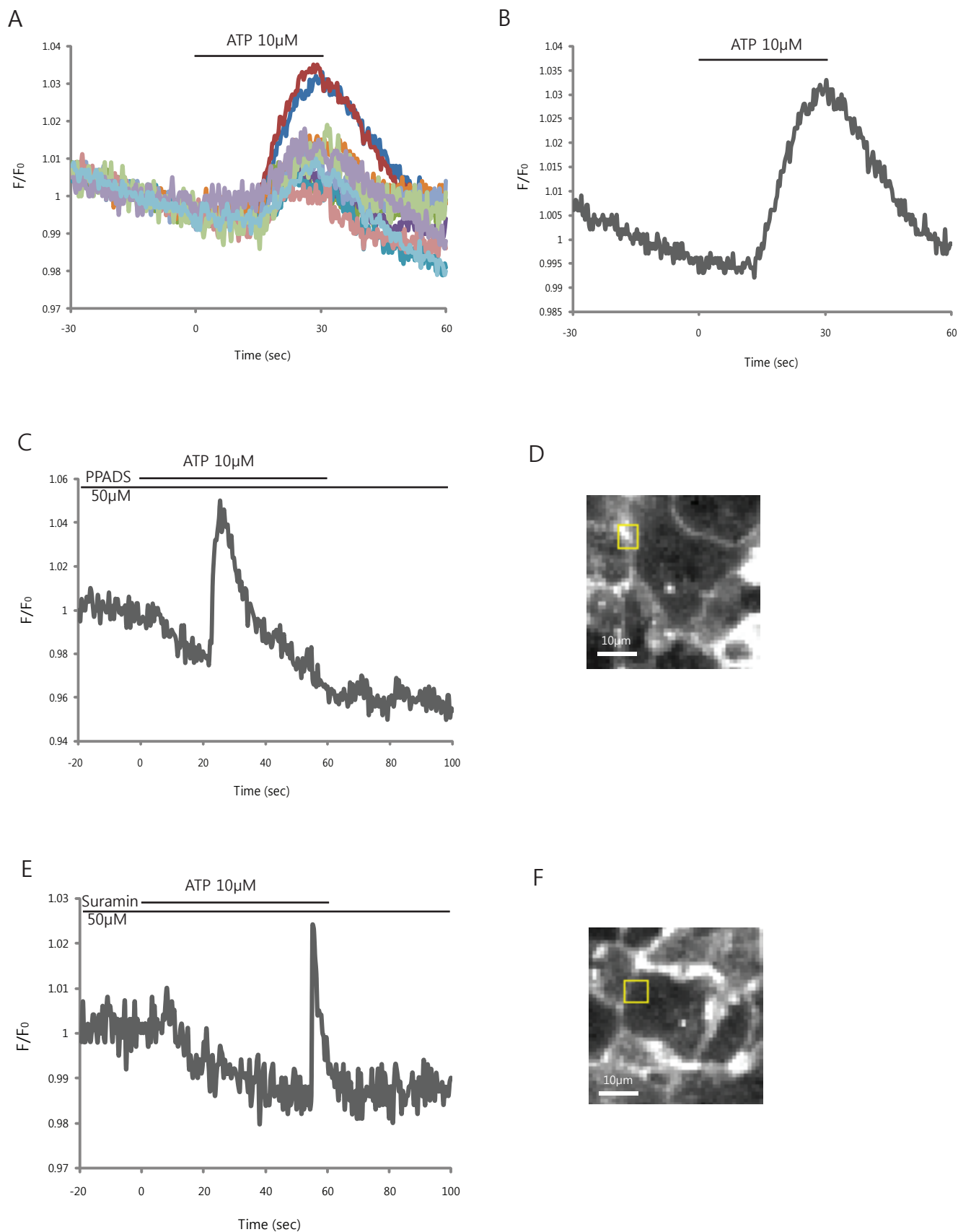


Fig. 9

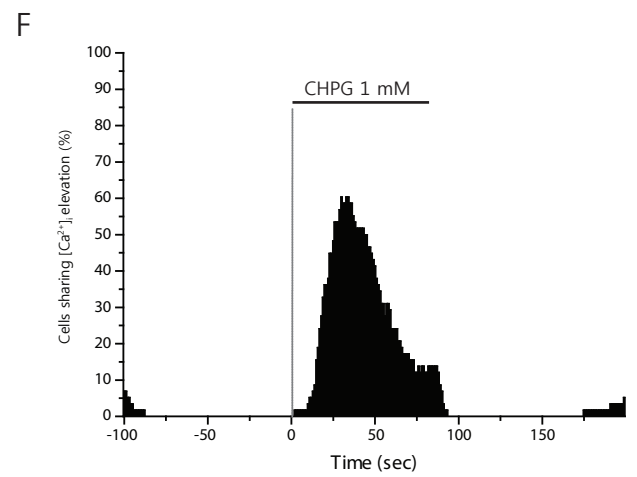
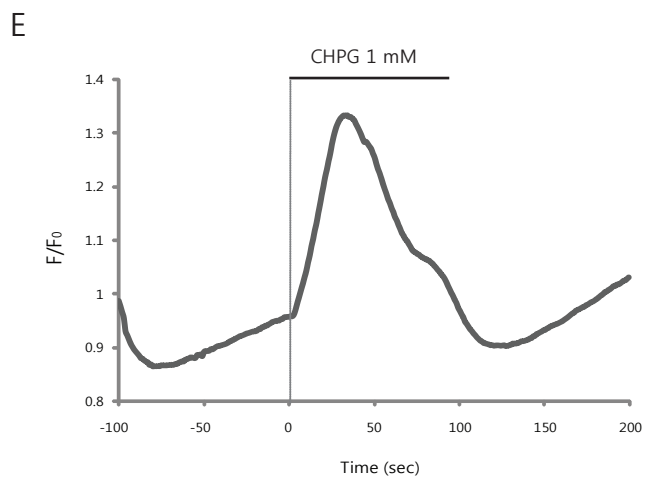
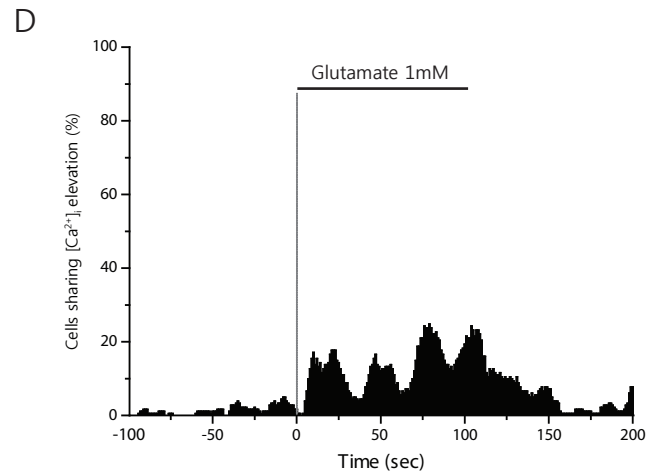
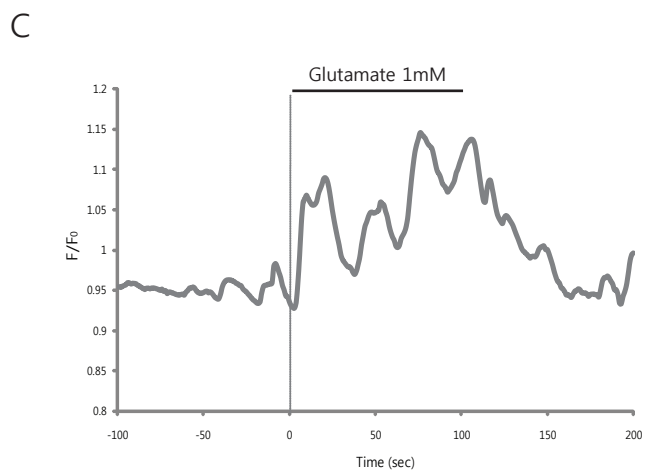
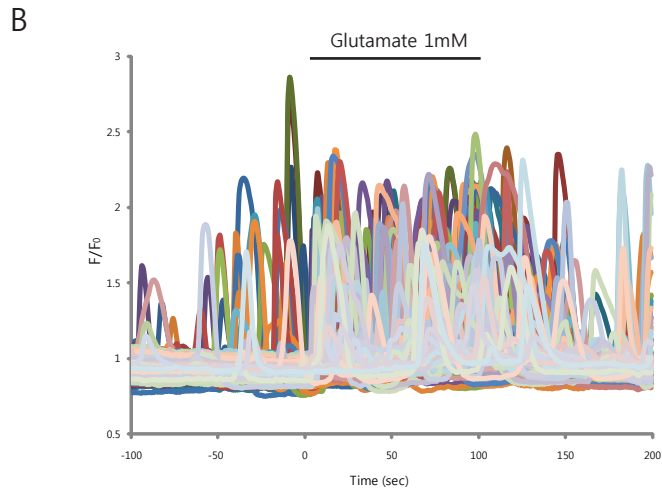
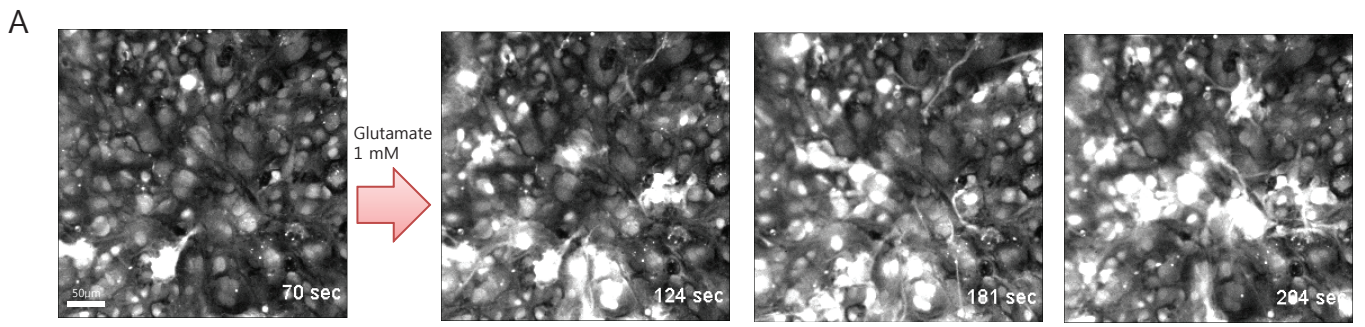


Fig. 10

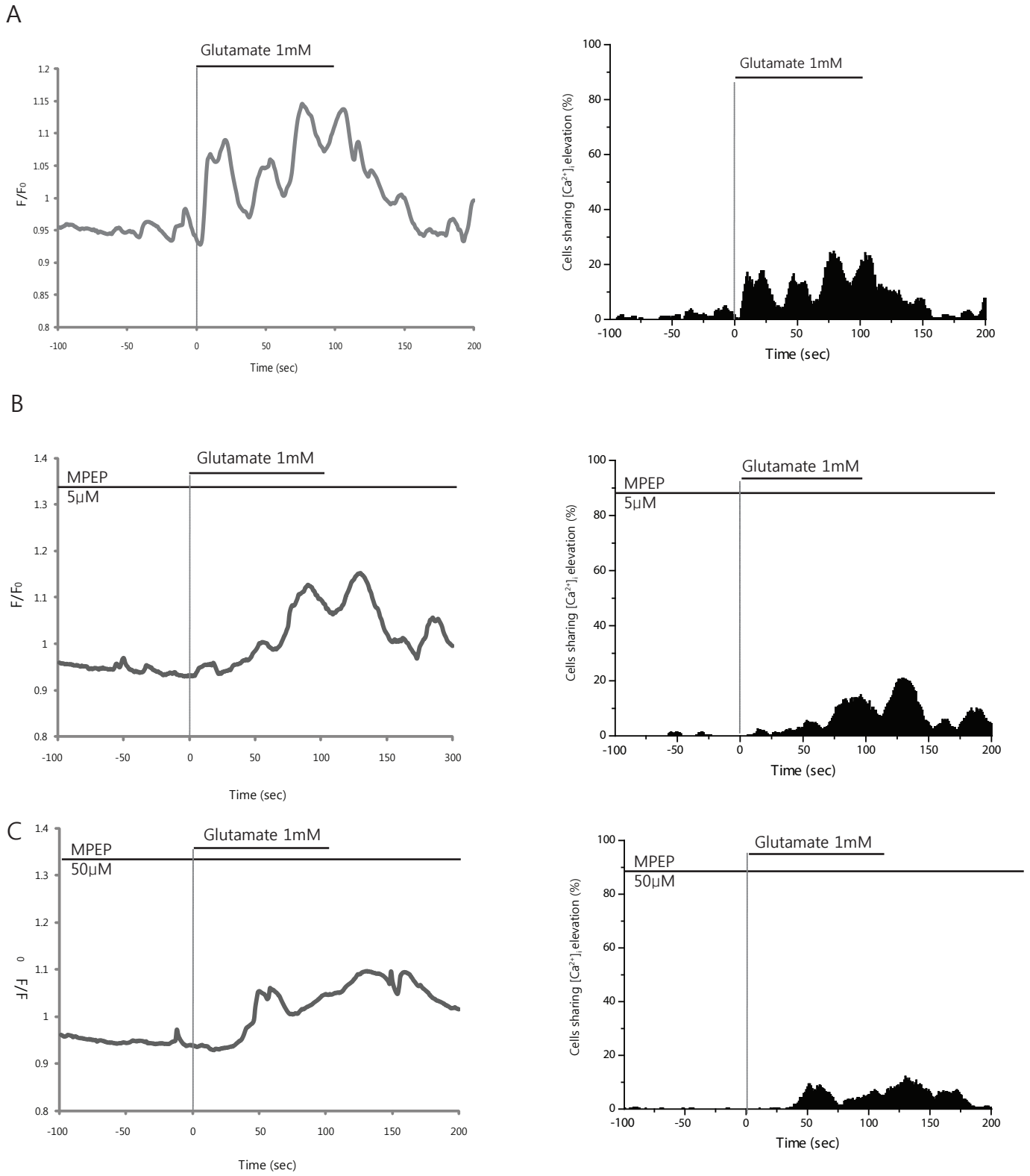


Fig. 11

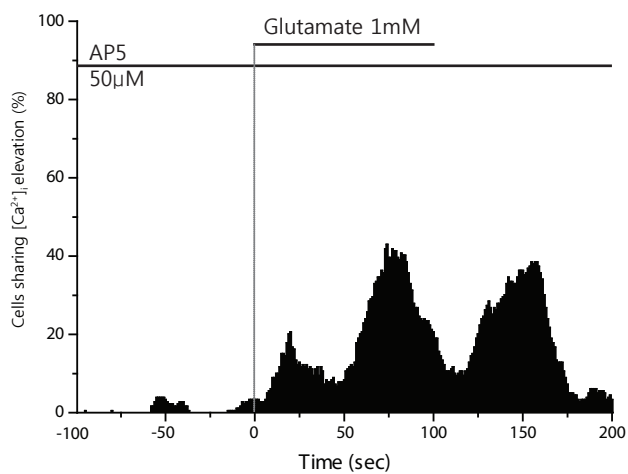
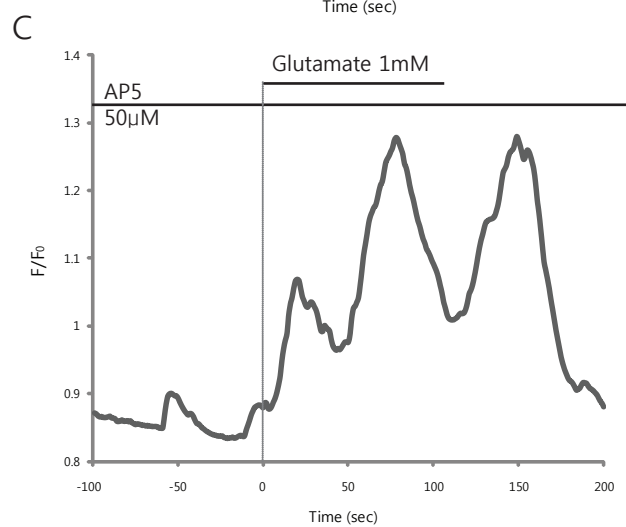
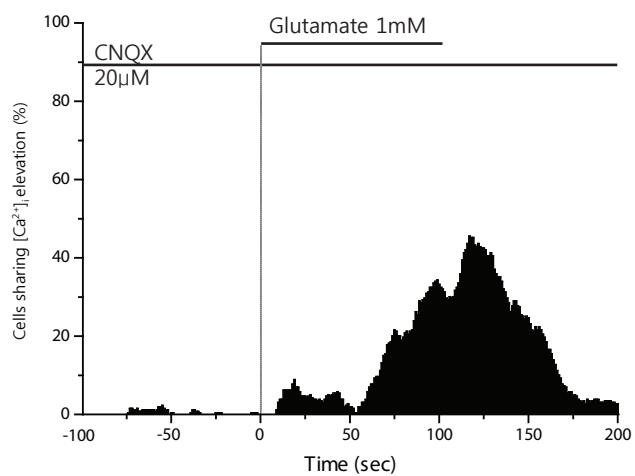
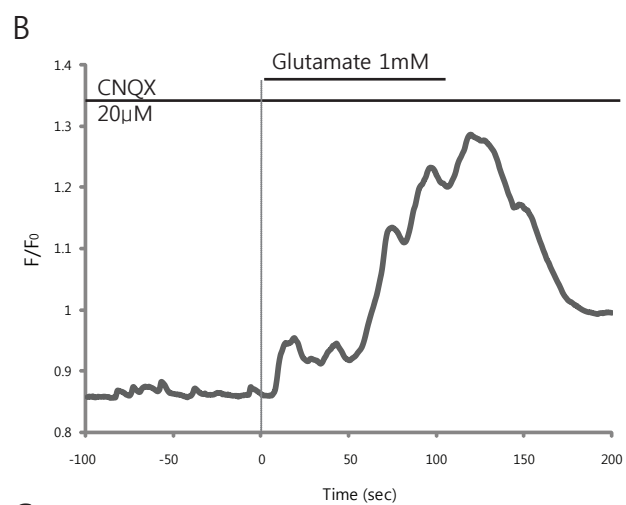
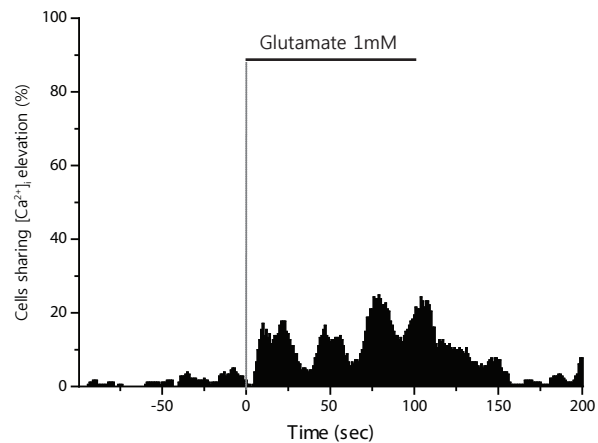
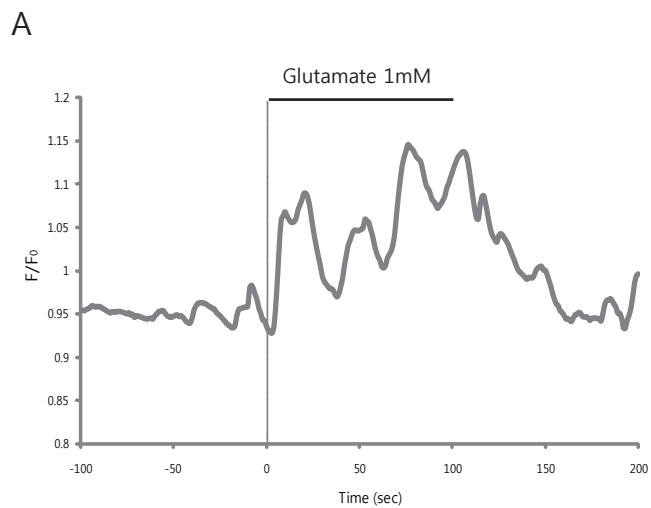


Fig. 12

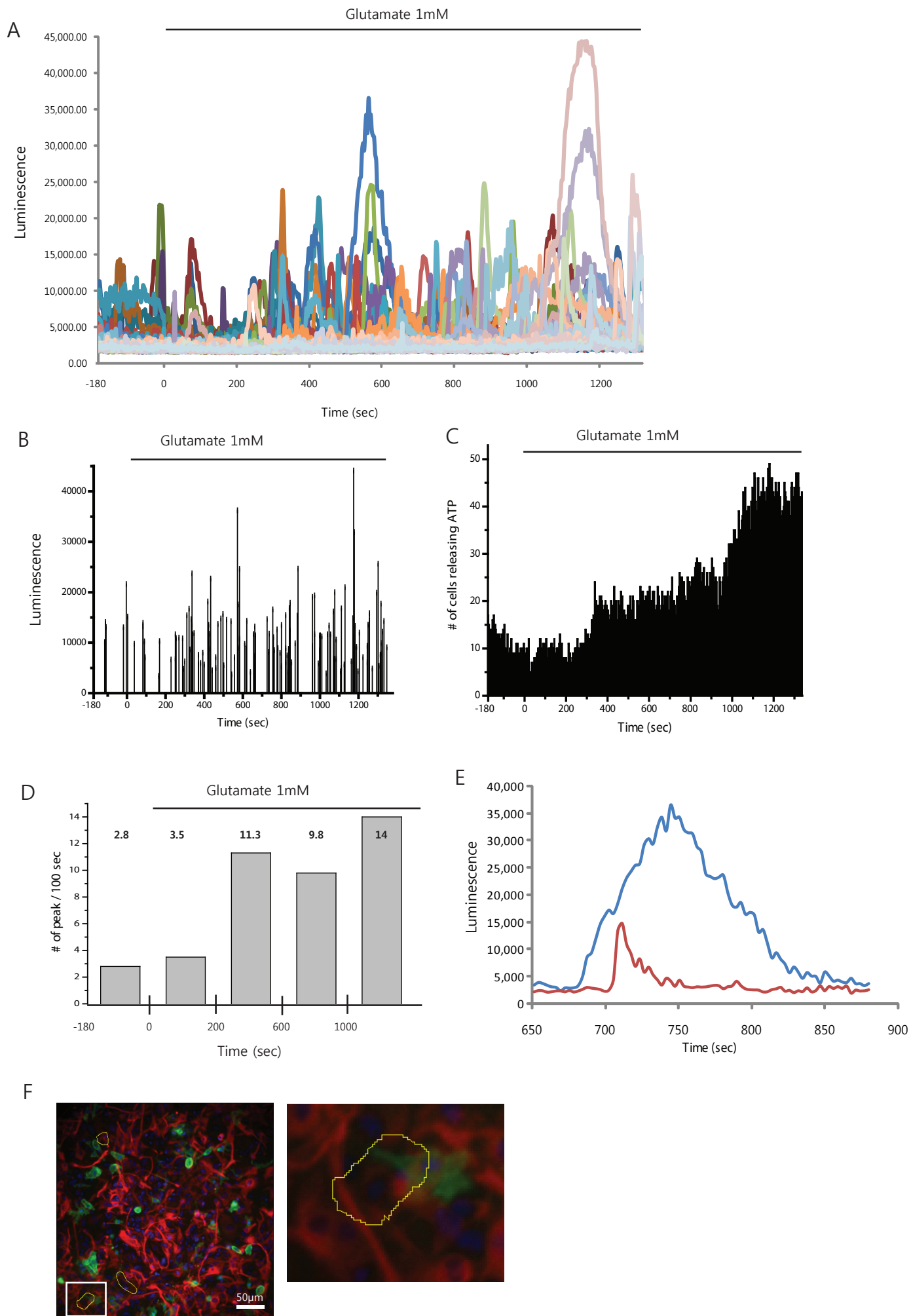


Fig. 13

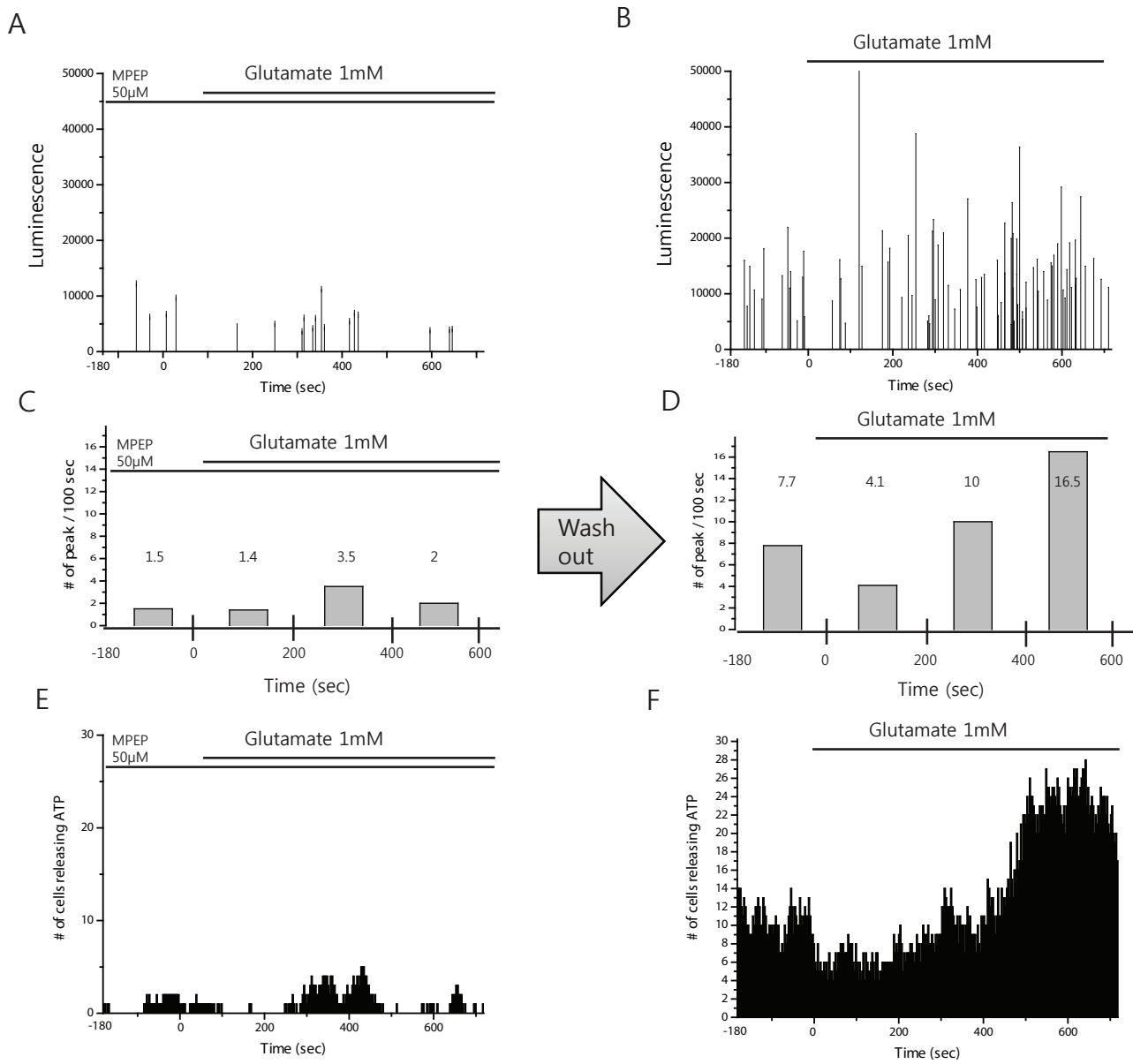


Fig. 14

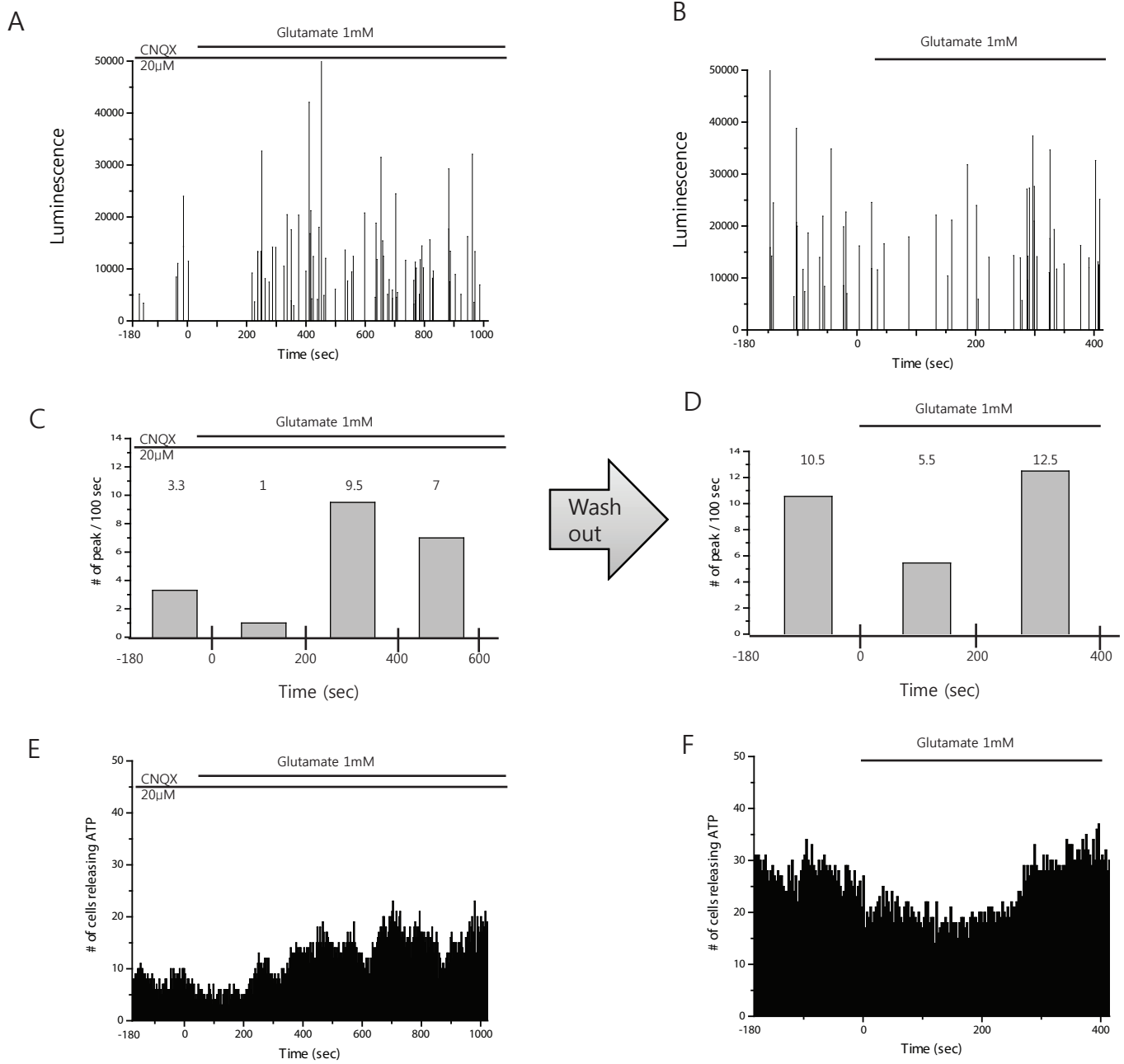


Fig. 15

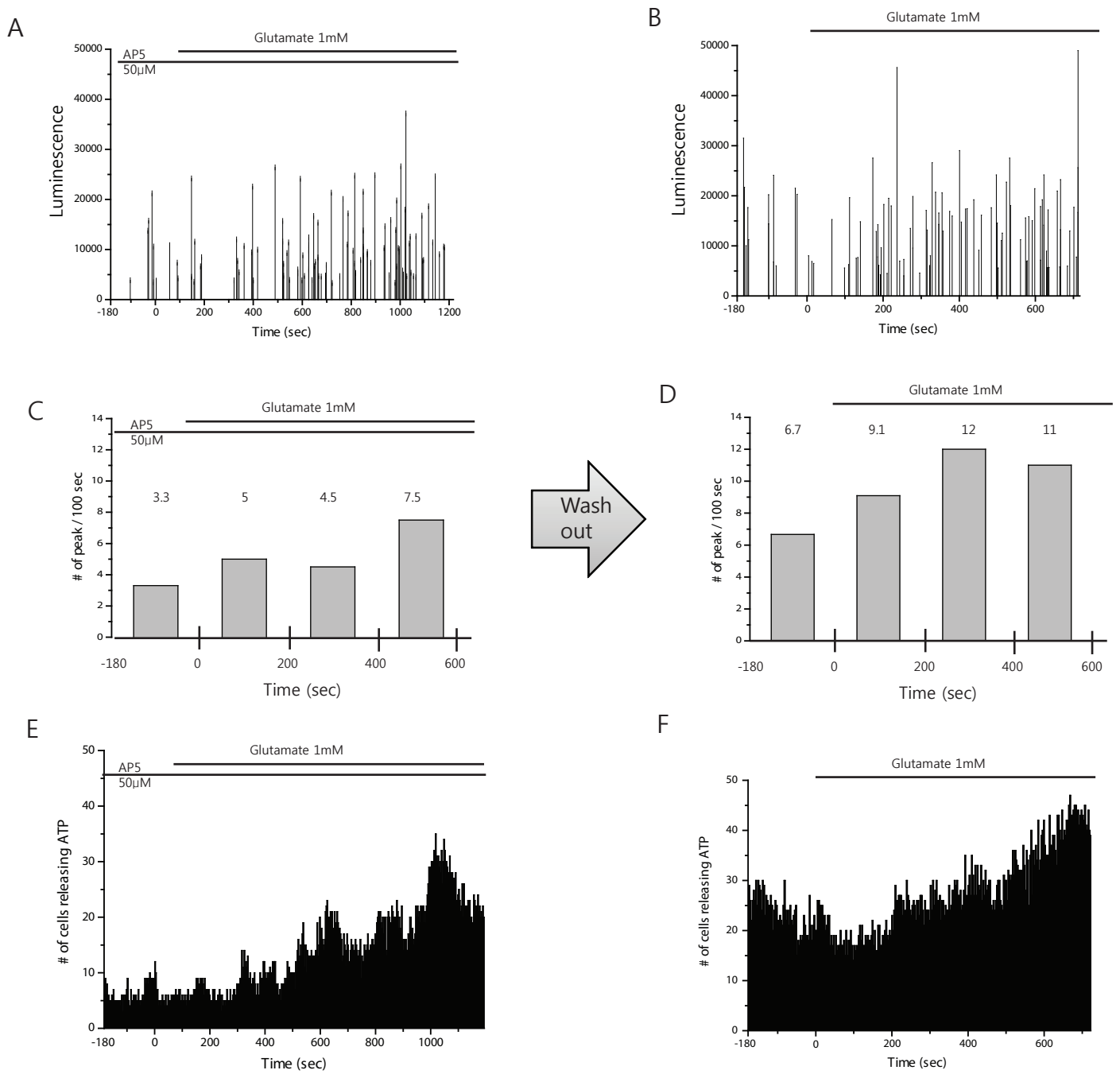


Fig. 16

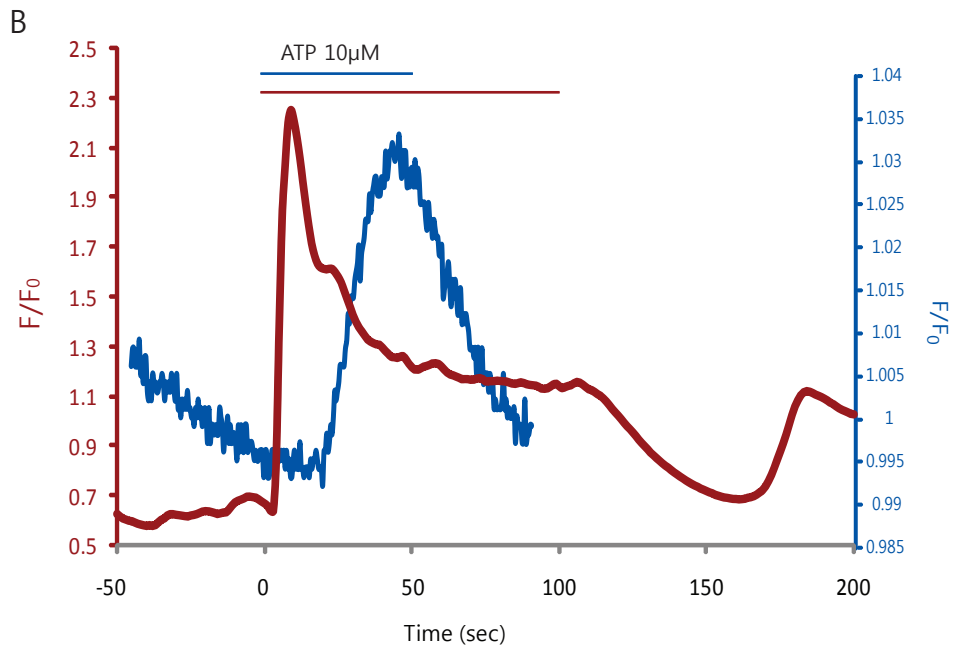
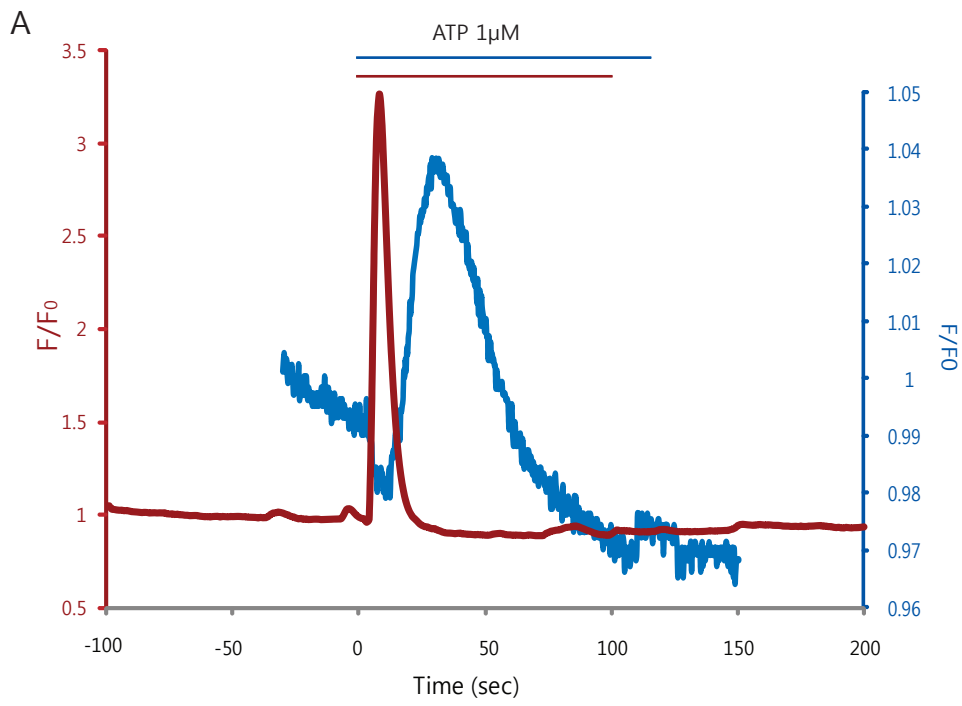


Fig. 17

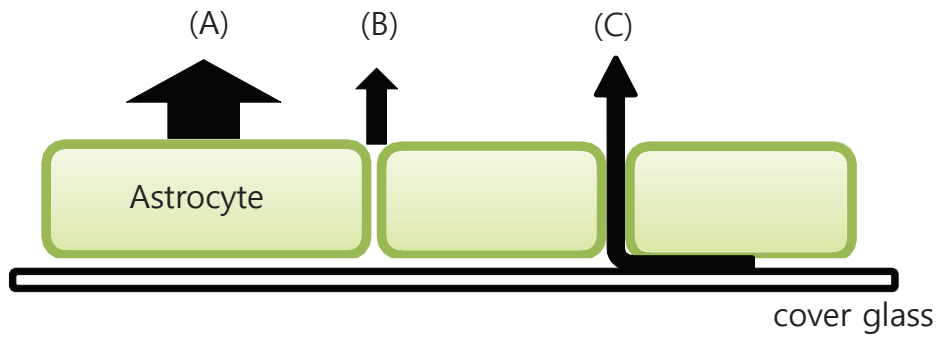


Fig. 18

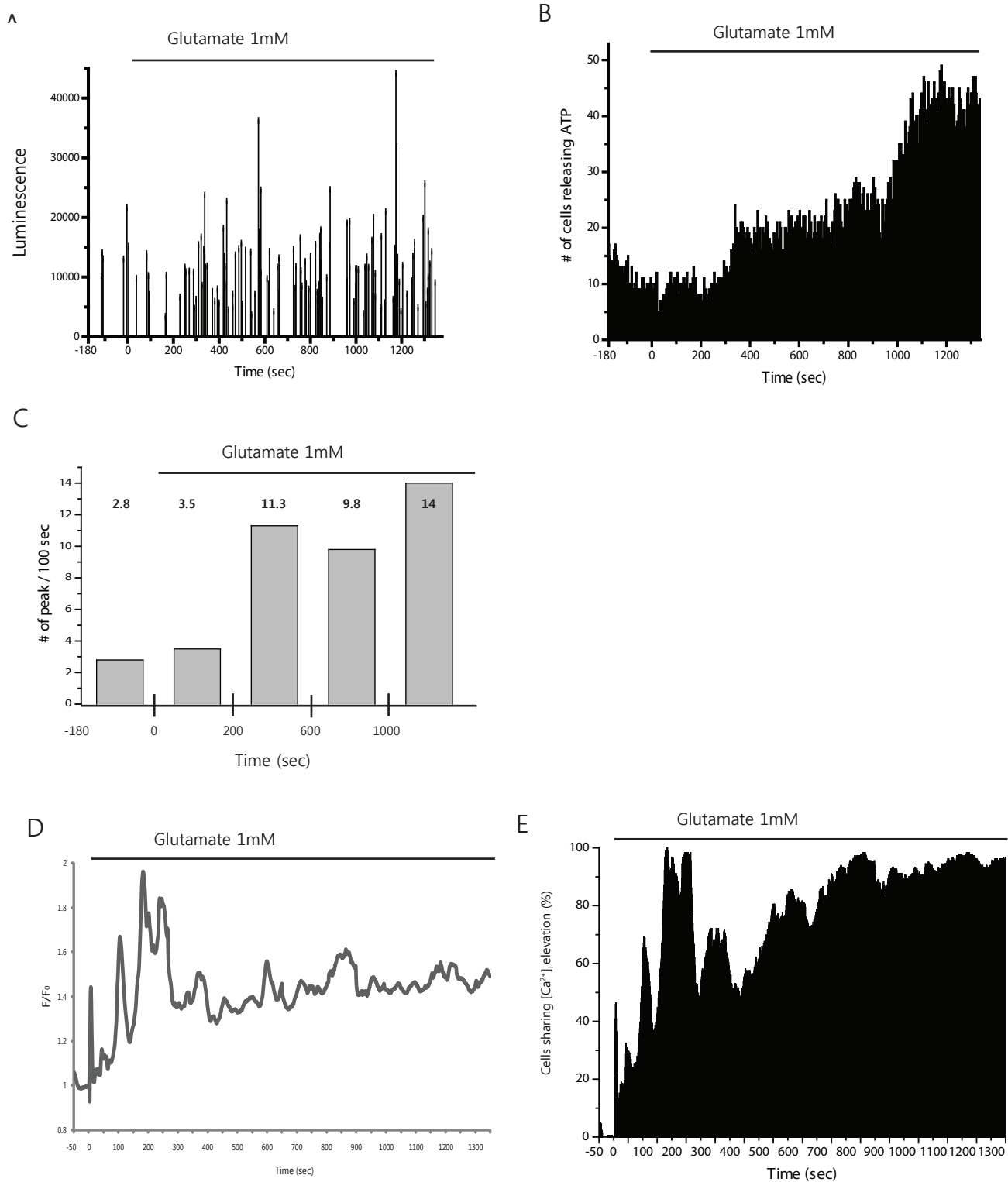


Fig. 19